ELSEVIER

Contents lists available at ScienceDirect

Journal of Archaeological Science

journal homepage: www.elsevier.com/locate/jas





Pompeian pigments. A glimpse into ancient Roman colouring materials

Celestino Grifa ^{a,b}, Chiara Germinario ^{a,*}, Sabrina Pagano ^{a,c}, Andrea Lepore ^{a,c}, Alberto De Bonis ^{b,d}, Mariano Mercurio ^{a,b}, Vincenzo Morra ^d, Gabriel Zuchtriegel ^e, Sophie Hay ^e, Domenico Esposito ^f, Valeria Amoretti ^e

- ^a Department of Science and Technology, University of Sannio, Benevento, Italy
- ^b CRACS, Center for Research on Archaeometry and Conservation Science, Naples, Italy
- ^c Department of Science of Antiquities, Sapienza University of Rome, Rome, Italy
- d Department of Earth Sciences, Environment and Resources, University of Naples Federico II, Naples, Italy
- ^e Archaeological Park of Pompeii, Naples, Italy
- f Institute of Classical Archaeology, Freie Universitat, Berlin, Germany

ABSTRACT

Pigments played a vital technological role by enabling the development of advanced artistic techniques, preserving cultural heritage through durable materials like frescoes and facilitating innovations in early chemistry, such as the creation of synthetic colouring compounds. This paper examines pigments found in some exceptional Pompeian contexts spanning the 3rd century BCE to the 79 CE eruption, covering almost the entire palette of an ancient painter made of natural and synthetic, inorganic and organic pigments.

Their composition has been revealed thanks to a non-invasive analytical approach designed to preserve these invaluable archaeological resources, illuminating that the artists skillfully mixed the colouring materials to achieve an uncountable range of colour tones.

Quantifying any individual colouring compound enables a review of recipes as reported by ancient sources and modern scientific literature and opens new scenarios in the artistic process that likely started in the *pigmentarium*. In the analysis of the mixtures, the role of Egyptian blue and red lead in the variation of shades, which are almost ubiquitous as additional components in paint mixtures, is worth noting. Ultimately, one of the samples uncovered the earliest known use of a light green compound containing baryte and alunite, providing the first definitive evidence of barium sulphate being utilized in the Mediterranean during ancient times.

1. Introduction

Pigments have always played an important role in human history as a means to convey artistic expression or, more simply, to leave a mark of their presence in a place.

In the course of history, the use and technology of pigments have evolved: in the past, man used the most readily available colouring minerals without any preparation or manipulation (earths); later on, ancient populations were able to obtain pigments through the selection and in some cases the transformation of natural resources, both of inorganic and organic nature.

The most striking examples, such as the synthesis of a blue pigment in ancient Egypt, the red and white Pb-based pigments used by Greek artists or the complicated process to produce Tyrian purple in Roman times, have been recounted by ancient scholars and are still being investigated by modern researchers.

Pompeian frescoes constitute a critical corpus for the study of Roman art, offering unparalleled insight into both the aesthetic practices and

the technical processes employed by artists in the Roman world. Preserved under volcanic ash following the eruption of Mount Vesuvius in 79 CE, these frescoes—found primarily in the urban centres of Pompeii and Herculaneum—serve as essential primary sources for understanding the material culture, socio-political structures, and artistic conventions of the ancient Roman elite. As examples of Roman wall painting, these works illuminate the evolution of artistic styles, technical innovations, and the socio-cultural functions of visual art within Roman society.

The study of Pompeian frescoes is indispensable for charting the development of Roman painting. The frescoes from Pompeii are classified into four distinct styles, each representing different stages of artistic progression. The First Style (or Incrustation Style), characterized by the simulation of marble panels, reflects early attempts at creating illusionistic effects. The Second Style (or Architectural Style) introduces more complex spatial illusions, with painted perspectives that give the illusion of three-dimensional space. The Third Style (or Ornate Style) emphasizes delicate, linear decoration, often incorporating mythological or idyllic themes, while the Fourth Style (or Intricate Style) combines elements from

E-mail address: chiara.germinario@unisannio.it (C. Germinario).

^{*} Corresponding author.

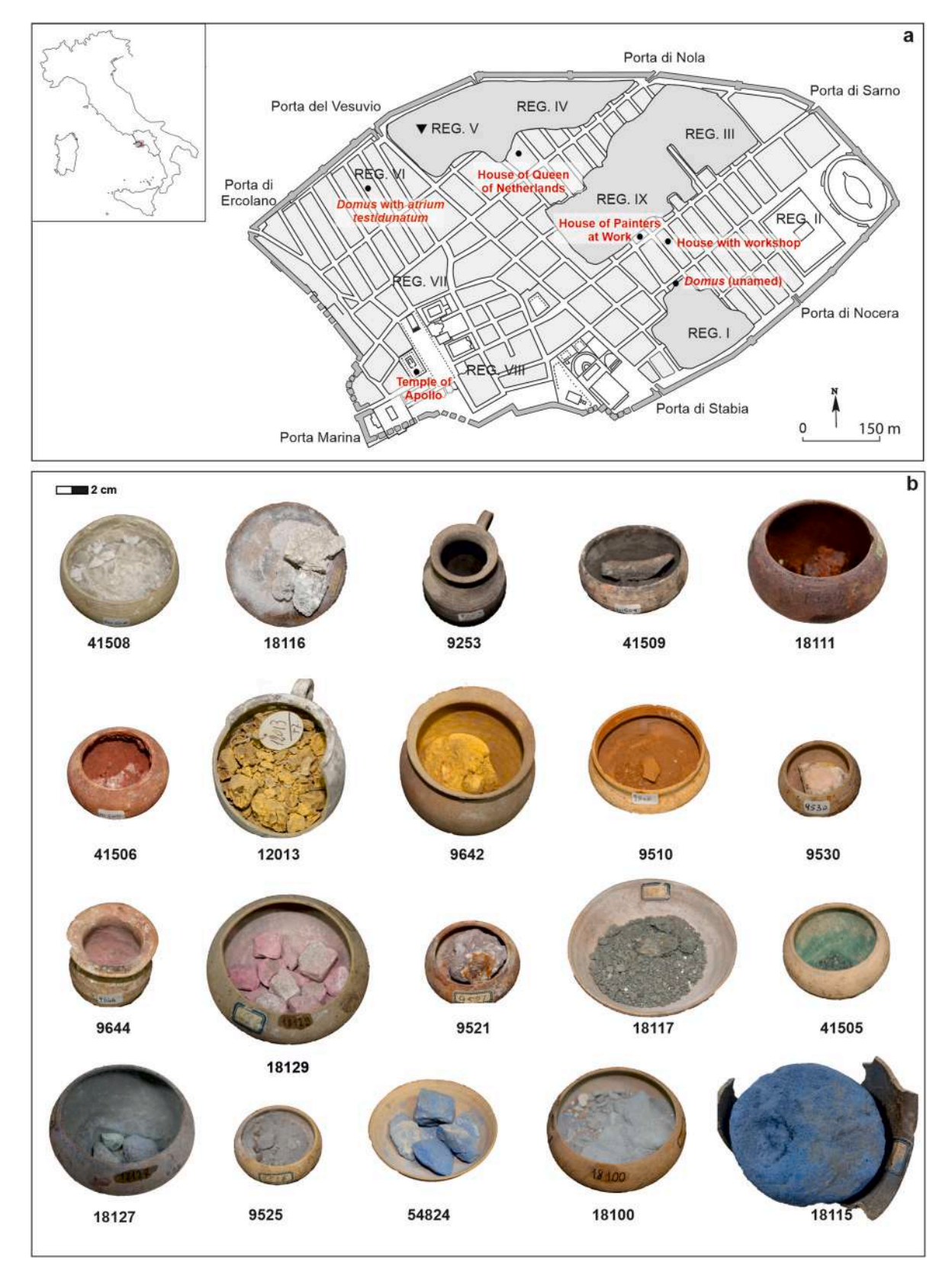


Fig. 1. a) Sketch map of Pompeii, in which there are reported the archaeological sites in which the pots were recovered; b) Images of some ceramic pots containing the analysed pigments.

ID Sample	Colour	Archaeological context	Age of archaeological context	Location			Storage	Reference
				Regio	Insula	Room		
18116/1629	white	-	-	_	_	-	Antiquarium, Inv. no.4	Augusti (1967)
41508	white	House of Painters at Work	1st CE	IX	12	9	_	=
9253	black	House with workshop	1st CE	I	9	9	Depository, Book no. 28	-
41509	black	House of Painters at Work	1st CE	IX	12	9	_	-
41506	red	House of Painters at Work	1st CE	IX	12	9	_	_
89128	red	Temple of Apollo	second half of the 2nd century BCE	VII	7	32	_	-
18111/1639	red	_	_	_	-	_	Antiquarium, Inv. no.4	Augusti (1967)
9642	yellow	House with Workshop	1st CE	I	9	9	Depository, Book no. 28	-
12013	yellow	Domus (unamed)	1st CE	I	18	2	_	-
DOD1	yellow	Domus with atrium testidunatum	first half of the 3rd century BCE	VI	11	11-12/7	_	-
9510	orange	House with Workshop	1st CE	I	9	9	Depository, Book no. 28	_
DOD2	orange	Domus with atrium testidunatum	first half of the 3rd century BCE	VI	11	11-12/7	_	_
9530	pink	House with Workshop	1st CE	I	9	9	Depository, Book no. 28	Giachi et al. (2009)
9644	pink	House with Workshop	1st CE	I	9	9	Depository, Book no. 28	-
18129/1644	pink	_	_	_	_	_	Antiquarium, Inv. no.4	(Augusti, 1967; Clarke et al., 2005; Giachi et al., 200
CAS1	pink	House of Painters at Work	1st CE	IX	12	2	_	_
9521	violet	House with Workshop	1st CE	I	9	9	Depository, Book no. 28	_
18100/1614	blue	_	_	_	_	_	Antiquarium, Inv. no.4	(Augusti, 1967; Giachi et al., 2009)
54 824	blue	Home of Queen of Netherlands	_	V	3	7	_	_
18115	blue	_	_	_	-	_	Antiquarium, Inv. no.4	-
89129	blue	Temple of Apollo	second half of the 2nd century BCE	VII	7	32	_	-
CAS2	blue	House of Painters at Work	1st CE	IX	12	2	_	_
9525	grey	House with Workshop	1st CE	I	9	9	Depository, Book no. 28	_
18127/1637-4	grey	_	-	_	_	_	Antiquarium, Inv. no.4	Augusti (1967)
41505	green	House of Painters at Work	1st CE	IX	12	9	_	Marcaida et al. (2018)
18117/1626	dark green	_	_	-	_	_	Antiquarium, Inv. no.4	(Augusti, 1967; Giachi et al., 2009)

previous styles, introducing greater complexity and the use of continuous architectural space to blur the boundary between the painted and real world (Salvadori and Sbrolli, 2021). These stylistic shifts indicate evolving aesthetic preferences and advancements in the technical execution of fresco painting, including the mastery of linear perspective, the manipulation of light and shadow, and the use of natural pigments to achieve vivid colour saturation. To achieve this high artistic expression, the painters had available a wide range of colouring materials (Siddall, 2006), for which decades of studies tried to explore their composition and provenance.

The object of the present paper is the analytical examination of 26 pigments, most of which are contained in their original pots (Fig. 1; Table 1); some are preserved in the Laboratory of Applied Research at the Archaeological Park of Pompeii, others were recently discovered in new excavations in the ancient city. We designed a combined noninvasive analytical approach aimed at the preservation of this outstanding heritage, but in the meanwhile, we tried to obtain information beyond the chemical-mineralogical composition of the pigments, pointing to the preparation process of the pigment before the final application on the mural paintings of Pompeian houses.

1.1. Archaeological contexts

The contexts in which these pots were found (Table 1) are known in the history of the city as examples of material culture associated with artists and wall paintings, and most of these exceptional finds are probably related to the extensive program of redecoration that took place at these specific sites (and across most of the city) after the earthquakes of 62–63 CE and later. Others are even more remarkable because they testify to the work of painters from earlier periods, as in the case of the Temple of Apollo and the *Domus* with *atrium testidunatum*.

Among the contexts that were active just before the 79 CE eruption, the first is the House with Workshop (I 9, 9) (Borgard et al., 2003), in which Della Corte noted 150 pots containing pigments in the front room of the house (Della Corte, 1965). Eschebach (1993) describes the workshop property of I 9,9 as being the residence of a 'pigmentarius' where the largest cache of pigments in Pompeii was found. The 1952 excavation Quaderno also documents the presence of a wooden cupboard in the corner of the front room, of which only the imprint on a plaster cast survives but which, in addition to pots of pigments, contained tweezers, spoons, knives, scales, stone pestles, spatulas, a compass, a plumb bob, and a whetstone that strongly suggest that the front of the property was used as a painter's workshop. On the north and east walls of this entrance room were two sets of vertical tally marks: one group in charcoal and the other in red gypsum, presumably recording quantities relating to the activities of the workshop. Subsequent excavations by Tuffreau-Libre found evidence of pits relating to the mixing of paints and even a painter's palette—a reused ceramic fragment—confirming that the property was involved in the manufacture of pigments and possibly the production of paintings (Tuffreau-Libre et al., 2014; Varone, 1995).

Other samples come from the *Insula* of Chaste Lovers (IX, 12), in particular from the House of the Painters at Work (IX 12, 9) (Varone, 1995; Varone and Béarat, 1996), whose name derives from the presence of several pigment pots in different rooms of the *domus* and an imprint of the basket used by the painters to transport the pots of pigments to their place of work. The House of the Painters at Work was partially excavated in the 1980s, and in a large salon, there was clear evidence that the decoration of this room had been interrupted by the eruption in 79 CE (Varone, 1995). Unfinished decorative schemes allow us to understand the process by which the teams of painters worked: working from the top down in strips, some of the lower registers remain blank, and only preparative sketches in *sinopia* can be seen that mimic the painted architectural elements already completed (Esposito, 2017). On the north wall, the main decorative scheme had been completed, and an artist was working on the remaining central framed panel; the presence of *sinopia*

sketches revealed this was to be a figurative scene. At the foot of the east wall, an assortment of instruments associated with painting were found alongside about 50 small ceramic pots containing pigments of colours corresponding to the room's colour scheme, including four different shades of white.

Recent excavations carried out on the northern-western part of the House unearthed other rooms in which quadrangular structures, interpreted as furniture, were discovered.

Interestingly, in the remains of the furniture discovered in room 2, among the traces of the shelves, a layer of blue pigment was found covered by a ceramic lid that lay in direct contact with the cinerite, as well as blurred residues of a pink pigment (Figs. S1a-d).

Other contexts, in which painters were probably working, include the House of the Queen of Netherlands (V 3, 7), and an unnamed *domus* (I, 18, 2) where a pigment pot was found (Table 1). This *insula* is still buried by eruption material; however, the façade of the *domus* on *Via di Castricio* has been partially unearthed, and a pot with a yellow pigment was discovered.

A yellow pigment and remains of a bright red-orange colour (Figs. S1e and f) were unearthed in a more ancient context dating back to the first half of the 3rd century BCE, a *domus* with *atrium testidunatum* (VI 11, 11–12/7) which was redecorated in the late 2nd - early 1st century BCE. The yellow pigment was found in a ceramic pot discovered in a pit in the area of the *domus* occupied by a garden and a cistern in a later phase, while the red-range pigment was discovered along the southern portion of the east wall of the *atrium*, on the work surface in use during the redecoration (Ballet and D'Auria, 2024).

In addition, blue and red pigments contained in fragments of ceramic pots were also discovered in the well-known Temple of Apollo (VII 7, 32), dating back to the second half of the 2nd century BCE (Fig. S1g; Table 1).

Some of the pots on display in the *Antiquarium* of Pompeii (those corresponding to inventory no. 4; Table 1), on the other hand, have an uncertain provenance because all the documentation concerning their original contexts was lost as they were destroyed in the bombardment of World War II.

The pigments were selected for the study among hundreds following two sampling criteria: i) the different shades of the main colours and ii) avoiding the pots of those pigments already studied whose data have been reviewed. These pots, in fact, have always attracted the interest of researchers; most of the studies aimed at identifying the compounds in terms of minerals, amorphous and organic components (Augusti, 1967; Clarke et al., 2005; Cottica and Mazzocchin, 2009; Giachi et al., 2009). Consequently, these pots have undergone sampling that sometimes caused the definitive material loss.

In this paper, the present work serves a dual purpose: first, to enhance our understanding of the pigments used in Pompeian, and by extension, ancient Roman art, through a detailed, non-invasive, correlative analysis while also drawing comparisons with ancient textual and archaeological sources and; second, to illuminate the remarkable expertise of Roman painters in mixing and proportioning various raw materials to achieve a wide spectrum of nuanced shades, shedding light on the technical sophistication of their craft.

1.2. Materials and methods

The pigment samples in the pots were studied through a non-destructive analytical strategy based on the combined use of portable spectroscopic and microscopic techniques directly in the Applied Sciences Laboratory of the Archaeological Park of Pompeii. In fact, no sampling and no transportation of the object was allowed except for sample ref. 18127 for which a micro-sampling was required to perform XRD and SEM-EDS analyses.

The samples were observed via digital microscopy (DM), to explore the presence of single- or multi-components in each colour hue. Dino-lite digital microscopes with magnifications ranging between 20x-220x

and 400x - 470x, respectively, were used. They were equipped with a 5.0-megapixel colour CMOS sensor and built-in coaxial illumination and Flexible LED Control (FLC). DinoCapture 2.0 software was used to acquire the images.

Digital Image Analysis (DIA) was carried out by using ArcMap software on 3 DM micrographs (one component of ArcGIS used for supervised image processing and classification) in order to distinguish the areas and DM images featuring a specific colour (corresponding to a specific compound) to quantify them.

The class categories (and the training samples for each class category) for each colour were created by using the Training Samples Manager panel, whereas the assignment of each pixel to the created classes was carried out by Maximum Likelihood Classification tool. The Layer Properties dialog box allowed us to obtain the counts of each class, reported as percentages normalized to the counts of the indistinguishable and/or unclassifiable regions that were categorized in a specific class. The quantification of the different colouring compounds was carried out on those samples in which the particles were visually distinguishable to identify the class categories in which to associate the pixels.

On the same images, the grain size distribution (GSD) of the different components of mixtures was evaluated by using the ImageJ software, a public available Java-based image processing tool, by which the minimum Feret (mF) values were measured to calculate Krumbein ϕ (where $\phi=-log_2$ (mF)).

Chemical (and mineralogical) investigation was carried out by means of spectroscopic techniques. Fiber Optics Reflectance Spectroscopy (FORS) was performed in the spectral range 380–1050 nm by using a tungsten lamp (BPS101 Tungsten Halogen Light Source with a spectral range of 350–2600 nm, B&WTek, Inc.) and the detector grating Qmini Broadcom. The measuring head geometry was $45^\circ/0^\circ$. A B&WTek inc white plate (99 %) was used as a reference. On an area of 2 mm² three spectra were recorded (128 scans on average, measurement time 0.05 s). FORS permitted the acquisition of the colorimetric coordinates, setting the primary illuminant D65 and the standard observer CIE 10° .

Portable X-Ray Fluorescence spectroscopy (pXRF) was performed with a portable Bruker TRACER 5G spectrometer, for semi-quantitative chemical compositions of analysed samples. The spectrometer was

equipped with rhodium (Rh) target X-ray source, silicon drift (SSD) detector with a 20 mm^2 wide active area, graphene window and internal camera. On areas of 3 mm (spot diameter) analyses using a HighZ (30 kV, $15 \,\mu\text{A}$, 20s) and LowZ ($15 \,\text{kV}$, $16 \,\mu\text{A}$, 30s) preset were performed, for the comprehensive identification of elements with both high and low atomic number, respectively. The software ARTAX Spectra 8.0.0.476 (Bruker AXS Handheld, Inc.) was used to process the spectra.

Fourier Transform Infrared Spectroscopy (FTIR) was performed in Attenuated Total Reflectance (ATR) using a BRUKER Alpha FTIR spectrometer equipped with a diamond crystal, collecting spectra in the spectral range $4000 - 400 \ \text{cm}^{-1}$ at the resolution $4 \ \text{cm}^{-1}$ and $64 \ \text{scans}$ for each run.

Raman spectroscopy (RS) was carried out with hand-held spectrometer Bruker BRAVO equipped with charge-coupled device (CCD) detector, a double laser excitation (785 and 853 nm, Duo LASER TM) and Sequentially Shifted Excitation technology (patented SSE TM), for the mitigation of fluorescence phenomena. The spectra were recorded in the spectral range 178–3200 cm $^{-1}$. As for FTIR, the software Bruker Opus 7.2 was adopted for data acquisition and processing (i.e. baseline correction, smoothing).

X-ray powder diffraction (XRPD) was performed with a diffractometer Bruker D2 Phaser 2nd gen (CuK α radiation, 30 kV, 10 mA, scanning interval 4–70° 20, time per step 2 s, step size 0,02° 20, Lynxeye 1D model detector). Samples were prepared using a few milligrams of sample powder smeared on a zero-background holder.

Scanning Electron Microscopy coupled with Energy Dispersive X-ray Spectroscopy (SEM-EDS) was carried out by using a Zeiss EVO 15 HD VPSEM operating at 13 kV accelerating voltage to record images and construct EDS maps thanks to an Oxford Instruments Microanalysis Unit with Xmax 80 EDS detector. The analysed sample (ref. 18 127) was preliminarily mounted on aluminium specimen stub with double-sided tape and coated with a layer of gold with a Q150R ES Sputter Coater (Quorum Technologies, UK).

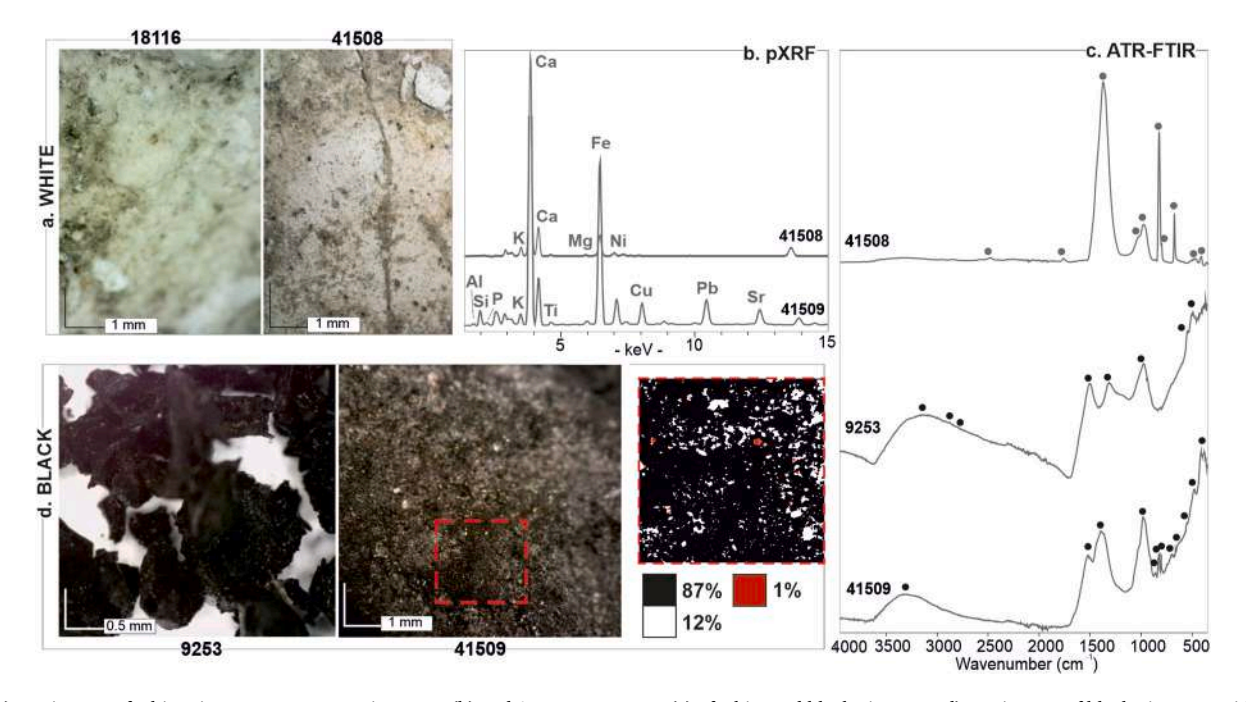


Fig. 2. a) DM images of white pigments. representative pXRF (b) and ATR-FTIR spectra (c) of white and black pigments. d) DM images of black pigments with results of DIA performed on a representative area of the sample ref. 41509.

Table 2Composition of pigments resulting by the analytical approach. The ancient name of each colouring compound was also reported.

ID Sample	Colour	Colour compounds				
		Ancient name	(Mineralogical) composition			
18116	White	Creta calcarea	Calcite			
41508		Paraetonium	Dolomite + aragonite			
9253	Black	Atramentum	Carbon black			
41509		-	$Carbon\ black + calcite + hematite + red\ lead + tenorite$			
41506	Red	Rubrica	Kaolinite + quartz + calcite + hematite			
89 128		Rubrica	Kaolinite + quartz + calcite + hematite			
18111		Sandyx (rubrica + cerussa usta)	Hydrated silicates + hematite + red lead + calcite + quartz			
9642	Yellow	$Ochrae + cerussa \ usta^{tr} + caeruleum^{tr}$	Goethite + kaolinite + calcite + red lead + cuprorivaite			
12013		$Ochrae + caeruleum^{tr}$	Goethite + kaolinite + calcite + cuprorivaite			
DOD1		Ochrae	Goethite + Pb-compounds (?)			
9510	Orange	Ochrae	Hydrated silicates + Fe-oxides and hydroxides + calcite + quartz			
DOD2		Sandaraca	Realgar			
18129	Pink	$Purpurissum + caeruleum + auripigmentum^{tr} + cerussa usta^{tr}$	Madder + carbonate-bearing $clay + cuprorivaite + red lead + orpiment$			
9644		Purpurissum + rubrica + cerussa usta	Madder + carbonate-bearing $clay + hematite + red lead$			
CAS1		Cerussa + rubrica	White lead + hematite + organic compounds (?)			
9530		$Creta\ argentaria + rubrica + cerussa\ usta$	Diatomaceous earth + hematite + red lead			
9521	Violet	Rubrica + cerussa usta $+$ $creta + caeruleum + auripigmentum$	$He matite + red\ lead + calcite + aragonite + cuprorivaite + or piment + hydrated\ silicates$			
54 824	Pink	Caeruleum	Cuprorivaite + quartz + calcite			
18115		Caeruleum	Cuprorivatite + quartz + calcite + aragonite			
18100		Lomentum (caeruleum + creta + auripigmentum + cerussa tr)	$Cuprorivaite + quartz + calcite + aragonite + orpiment + white lead^{tr}$			
89129		Caeruleum	Cuprorivaite + quartz + calcite			
CAS2		Caeruleum	Cuprorivatite + quartz + calcite			
9525	Grey	Caeruleum + creta + rubrica + cerussa usta $+$ auripigmentum	$Cuprorivaite + calcite + aragonite + hematite + red \ lead + or piment$			
18127		-	$Baryte + quartz + cuprorivaite + clayey \ minerals + alunite + calcite^{tr}$			
41505	Green	Chrysocolla	Malachite			
18117	Dark green	${\it Creta\ viridis} + {\it caeruleum} + {\it cerussa\ usta} + {\it auripigmentum}$	$Green\ earth + cuprorivaite + red\ lead + or piment$			

2. Results

2.1. White

Two white pigments labelled 18116 (*Antiquarium*) and 41508 [House with Workshop (19, 9)] were analysed. The sample ref. 18116, in shapeless pieces, presents a fine-sandy aspect, whereas the sample ref. 41506 appears more compact and uniformly fills the vessel (Fig. 1).

Sample 18116 is a whitish-yellowish mixture ($L^* = 97.33$; $a^* = 0.73$; $b^* = 6.65$; Table S1) containing grey and brown spots and small yellow particles. On the other hand, the colour of sample 41508 has a darker appearance ($L^* = 87.07$; $a^* = 0.33$; $b^* = 6.35$) because of the presence of deposited materials in the pot (i.e., ash); however, it appears as a mixture including rare black particles and yellow spots (Fig. 2a).

The sample ref. 18116 has Ca as a predominant element (Fig. S2), along with lower amounts of Si and Fe particles; moreover, the FTIR spectrum (Fig. S2) shows the typical bands of calcite (2507, 1795, 1398, 872, 712 cm⁻¹) as confirmed by RS (1085, 711 cm⁻¹) (Fig. S3). This calcite-containing white pigment has already been documented among the Pompeian pots (Augusti, 1967; Giachi et al., 2009), corresponding in composition and appearance to the pigment referred as *creta calcarea* (Table 2), specifically reported by historical sources as *melinum* or *selinusa* (Augusti, 1967; Morgan, 1960; Rackham, 1968).

On the other hand, the sample ref. 41508 has the typical infrared bands of dolomite (2537, 1815, 1427, 878, 729 cm⁻¹) which account for the prevalent Ca and subordinate Mg detected via pXRF (Table S1). However, it is worth to note the presence of aragonite, highlighted by the peak at 854 cm⁻¹ in FTIR spectrum (Izzo et al., 2020) (Fig. 2c). In the latter, the peaks at ca. 1080, 1035, 523 and 466 cm⁻¹ and lower concentration of Si suggest additional presence of silicates. Moderate amounts of Si and Fe are also present (Fig. 2b; Table S1).

Thus, the data indicate that dolomite is the main constituent of the pigment, according to published literature reporting such a carbonate as one of the most attested white pigments in Pompeii (Fagnano et al., 2003; Giachi et al., 2009; Marcaida et al., 2018; Varone and Béarat, 1996). The historical sources (Morgan, 1960; Rackham, 1968) also recount that white pigment was commonly obtained by using carbonates as pure compounds or mixtures of two components varying in their

percentages. Dolomite, huntite (Aliatis et al., 2011; Baraldi et al., 2002; Fagnano et al., 2003), aragonite (Augusti, 1967; Varone and Béarat, 1996), and the relative mixtures with calcite (Augusti, 1967; Baraldi et al., 2002; Fagnano et al., 2003; Giachi et al., 2009), in fact, were currently detected in the white pigments of Pompeii. Along with the creta calcarea, in fact, Pliny describes the paraetonium (a white shelly calcium carbonate pigment) as the "natural, austere colour" (Rackham, 1968), occasionally found in blocks carrying the inscription ATTIORU (M) referred to colour factory in Pompeii (Augusti, 1967; Baraldi et al., 2002), in which, curiously, Aliatis and co-authors (Aliatis et al., 2011) detected huntite (Aliatis et al., 2011). Nonetheless, other substances have been found in Pompeii, also in a mixture with other pigments. Among them, creta silicea (natural earth pigment containing clay minerals as main compounds) (Augusti, 1967; Giachi et al., 2009) and cerussa (a manmade white composed of Pb-carbonate) (Baraldi et al., 2002; Fagnano et al., 2003; Varone and Béarat, 1996), recovered as pure white pigment or additional compound in other colour to obtain different nuances.

2.2. Black

Two different black pigments coming from House with Workshop (ref. 9253) and the House of the Painters at Work (ref. 41509) were investigated, inferring a different nature of colouring materials (Fig. 1).

A dark hue characterises the sample ref. 9253 (L* = 20.29; a* = 0.37; b* = 5.39); it appears as a very cohesive flake with irregular shapes and a shiny appearance (Fig. 2d). pXRF analysis measured Ca and Fe as the most abundant elements, along with moderate amounts of P and K (Table S1); meanwhile, the two main peaks at 1570 and 1319 cm $^{-1}$ of Raman spectrum attributable to carbonaceous materials (Coccato et al., 2015) (Table S1) revealed the organic origin of the pigment. Accordingly, the FTIR spectral evidence is consistent with a pigment from the black carbon group, probably flame charcoal prepared with soot obtained from burning resinous wood (Tomasini et al., 2012b). The FTIR spectrum (Fig. 2c) shows a broad band at ca. 3200 cm $^{-1}$ (O–H stretching mode), weak peaks at 2925 and 2845 cm $^{-1}$ (aliphatic C–H stretching), and broad bands at 1555, 1370, 1237 (aromatic ring vibrations and aliphatic methylene and methyl groups, respectively) and 1027 cm $^{-1}$

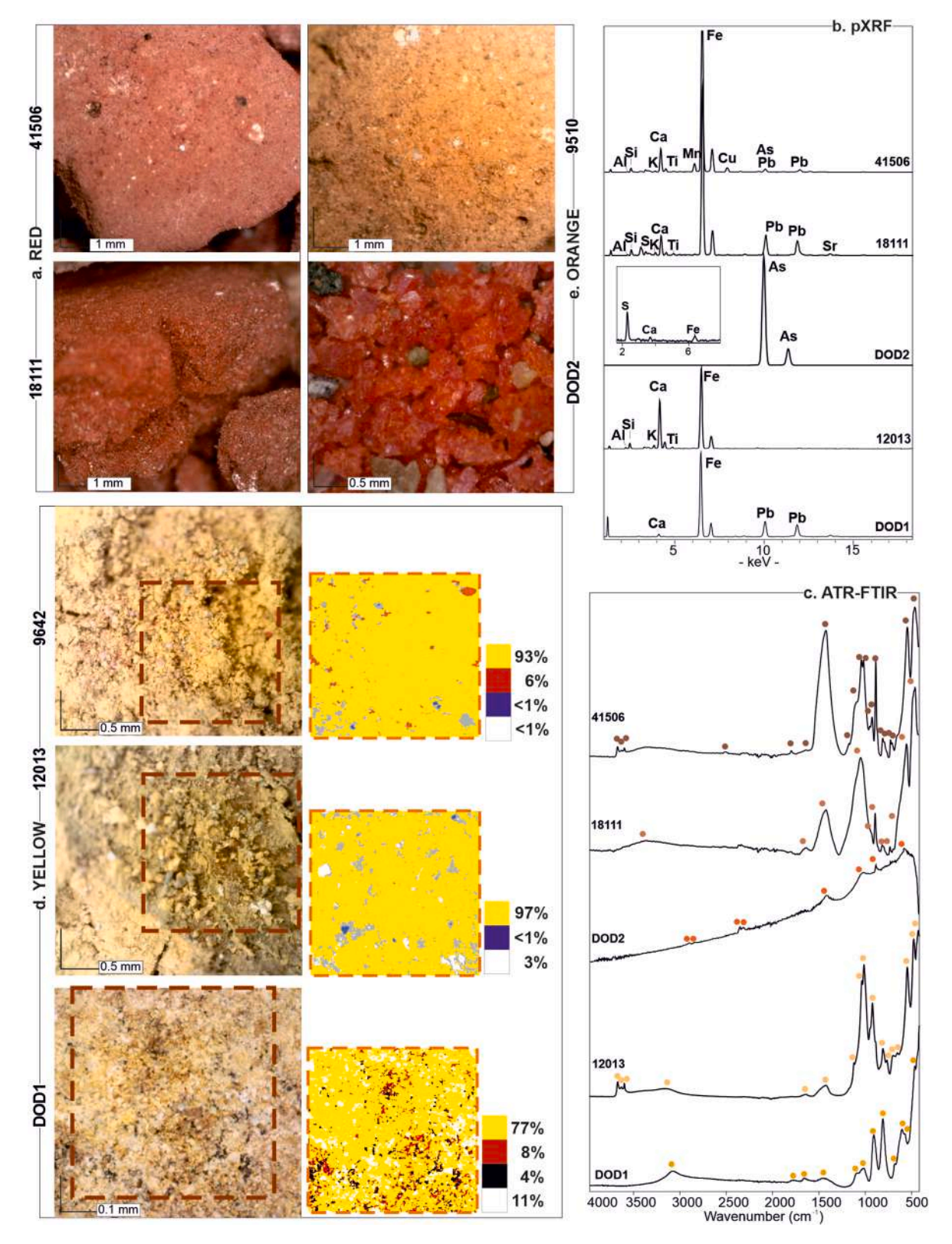


Fig. 3. a) DM images of red and orange pigments. Representative pXRF (b) and ATR-FTIR (c) spectra or red, orange and yellow pigments. d) DM images of yellow pigments and results of DIA performed on representative areas. (For interpretation of the references to colour in this figure legend, the reader is referred to the Web version of this article.)

(C–O stretching of aryl ether) (Tomasini et al., 2012a). The presence of potassium by pXRF supports this hypothesis since K occurs in the pigments obtained by the carbonisation of wood (Tomasini et al., 2012a). However, the occurrence of phosphorous, as well as the shift of the band

in the region $1100\text{-}1000~\text{cm}^{-1}$ toward the lower wavenumber with respect to the reference material, could be indicative of the possible addition of some bone black compounds to the colouring mixture (Tomasini et al., 2012a).

This pigment can be identified as *atramentum* (Table 2), an artificial pigment obtained by burning resins or resinous wood, as reported by the historical sources (Augusti, 1967; Morgan, 1960; Rackham, 1968).

The sample ref. 41 509 appears compact with blackish mixture gradually bleeding in a dark reddish shade containing tiny (ca. 0.03 mm) white (ca. 12 %) and red particles (ca. 1 %), which increase the colorimetric values measured via FORS (L* = 49.88, a* = 1.89, b* = 7.36; Table S1).

Unfortunately, in this case, the spectroscopic techniques did not give clear information; the high fluorescence effect affects the Raman spectrum and FTIR only displays the bands of calcite (1440, 875, 854, 712 ${\rm cm}^{-1}$) (Fig. 2c). More informative was pXRF that measured predominant Ca and Fe, along with moderate Pb and Cu (Table S1; Fig. 2b).

Thus, the nature of such a pigment appears more complex; by trying to combine microscopic and scarce spectroscopic and chemical information, it was possible to provide a tentative composition of the mixture. In particular, the black mixture, likely of organic nature, was mixed with: a) (white) calcite, as suggested by its diagnostic infrared peaks and the presence of Ca, b) (red) Fe- and Pb-oxides, c) minor tenorite, as already reported by Giachi and co-authors (Giachi et al., 2009) who studied the same pot, which might justify the presence of Cu.

2.3. Red

Two shades of red were analysed (Fig. 3a); the sample coming from the House of the Painters at Work (ref. 41506) is lighter (L* = 43.39; a* = 20.60; b* = 17.93) and appears as a fairly homogeneous red mixture with white grains and rare black and yellow particles (Fig. 3a). The darker shade of sample ref. 18111 (*Antiquarium*) (L* = 52.67; a* = 26.64; b* = 25.72) is more cohesive and shows less black and white particles (Fig. 3a).

In the light red shade (ref. 41 506), FTIR detected diagnostic peaks of kaolinite (3693, 3651, 3619, 1630, 1164, 1029, 1006, 973, 912 cm $^{-1}$), quartz (798, 778, 696 cm $^{-1}$) calcite (1795, 1417, 872, 712 cm $^{-1}$) and iron oxides (528, 443 cm $^{-1}$) (Fig. 3c), identified as hematite via RS (410, 500, 616 cm $^{-1}$) (Germinario et al., 2021) (Table S1). Data from vibrational spectroscopy reflect the presence of predominant Fe detected via pXRF, followed by Ca and moderate amounts of Mn, Cu, Si, and traces of As (Fig. 3b). In addition, the FORS spectrum has the characteristic S-shape of red ochre (Fig. S4) with an increase of intensity from \sim 550 to \sim 600 nm and a shoulder at \sim 650 nm due to iron absorption (Marey Mahmoud, 2019).

This evidence allowed for the identification of this pigment as *rubrica* (red ochre) (Table 2), one of the most important and diffused red colours that Pliny classified in three types, namely *rubra*, *intermedia* and *minus rubens*, from darker to lighter red colour (Rackham, 1968).

The spectroscopic response of red ref. 89128 closely matches the FTIR spectrum of the sample ref. 41506, indicating the presence of kaolinite, iron oxides, quartz, and calcite (Table S1; Fig. S2). This similarity extends to the pigment's colour, observed in DM as a homogeneous mixture of red particles interspersed with white, blue, and yellow spots (Fig. S2).

On the other hand, the darker hue (ref. 18111) is featured by prevalent Fe, along with moderate amounts of Pb, Ca, Si, and K (Fig. 3b). Despite the presence of lead, FTIR only revealed the typical features of the red ochre, displaying the bands of hydrated silicates (3384, 1640, 1030 cm⁻¹), quartz (795, 779, 694 cm⁻¹) and calcite (1410, 873, 711 cm⁻¹) along with those attributed to iron oxides (525, 435 cm⁻¹) (Germinario et al., 2018a) (Table S1). Moreover, the characteristic spectrum with S-shape of red ochre was detected via FORS (Fig. S4).

In this case, the pigment could be associated to the *Sandyx*, a mixture of *rubrica* and *cerussa usta* (red lead, Pb₃O₄) (Arena, 2020; Augusti, 1967) (Table 2). The addition of Pb-based pigment to the red ochre can be attributed to two main reasons: 1) the willingness to obtain a more intense and brilliant nuance, 2) the need to lower the cost of the artificial *cerussa usta*, more expensive (6 denarii per pound) than the red ochre (2

denarii per pound) according to Pliny (Arena, 2020; Rackham, 1968).

The Pompeian red palette, however, also encompasses other red pigments that, unfortunately, we were not able to analyse because of the complete loss of material in their containers. In particular, previous studies reported the presence of the cinnabar (HgS) (*minium*) (Aliatis et al., 2011; Augusti, 1967; Cottica and Mazzocchin, 2009; Fagnano et al., 2003; Germinario et al., 2018b; Marcaida et al., 2018) and realgar (As $_2$ S $_2$) (sandaraca) (Augusti, 1967) as red pigments analysed in their pots or on the Pompeian wall paintings.

2.4. Orange

The pigment in the pot ref. 9510 unearthed in the House with Workshop appears as a compact fine-grained material, whose colorimetric coordinates (L* = 49.01; $a^* = 15.03$; $b^* = 27.26$; Table S1), in particular the L* value, may be influenced by some darker grains, thereby causing the return of a darker nuance compared to how it is visually perceived. DM highlighted an orange matrix with scattered white, yellow and brown particles. Additionally, traces of blue grains were also observed (Fig. 3a) associated with the presence of Cu as determined by pXRF (Fig. S2). Chemical analyses identified Fe as the major element, followed by minor amounts of Ca and Si (Table S1). FTIR revealed the bands of Fe-oxides (551, 465 cm⁻¹), hydrated silicates (3381, 1629, 1027, 631, 438 cm⁻¹), quartz (797, 781, 695 cm⁻¹) and calcite (1410, 873, 709 cm⁻¹) (Fig. S2) whereas RS only detected the peaks of hematite (411, 621 cm⁻¹) (Table S1). The reflectance spectrum coherently presents the typical S-shape of ochres, with a growth of the curve from \sim 550 to \sim 600 nm and the band at \sim 650 nm usually associated with the mixture of iron-based oxides and hydroxides (Fig. S4).

Few authors account for pots containing an orange colour (Augusti, 1967; Cottica and Mazzocchin, 2009; Varone and Béarat, 1996); our data highlighted the coexistence of yellow and red earth (*sil* and *rubrica*) or, more probably, the presence of natural, orange earth (*ochrae*) (Table 2), consistent with Cottica and Mazzocchin, Cottica and Mazzocchin, 2009), who reported a yellow-red pigment composed of goethite and hematite. The latter, with a disordered structure, was also detected in the House of the Painters at Work (Varone, 1995), where the different orange shades were obtained by using iron- and lead-based pigment (i. e., *cerussa usta*). Moreover, yellow-red Pb-based pigments from House with workshop (I 9, 9) were analysed by Augusti (1967) who identified the pigment that Pliny calls *spuma argenti*, namely the litharge (PbO) containing traces of Ag and obtained by the collection of the foam derived by the fusion of the natural mineral extracted by mines of silvery minerals (Augusti, 1967; Rackham, 1968).

From the ancient context of the *domus* with *atrium testidunatum* (VI 11, 12-12/7), instead, small pieces of a bright red-orange colour ($L^* = 55.41$; $a^* = 39.66$; $b^* = 46.07$; Table S1) were collected (sample DOD2). DM showed that they constituted of small, striated red-orange particles with a resinous lustre (Fig. 3a), occasionally showing tiny yellowish particles, providing a warm orange shade.

pXRF spectrum measured the predominance of As and S, along with lower Ca and Fe and traces of Ni (Table S1: Fig. 3b) and RS (Fig. S3) showed the Raman shifts at 352, 288, 219, 189 cm $^{-1}$ (Vermeulen et al., 2018) (Fig. S3; Table S1) univocally disclosing the nature of the pigment, as realgar (As₂S₂). Moreover, the FORS-VIS curve has the characteristic sharp increase in reflectance at ~530–600 nm with a weak absorption at ~700 nm (Fig. S4).

Realgar, namely the ancient *sandaraca* (Table 2) used as arsenic-based pigment in the ancient Pompeii (Augusti, 1967), was listed among the intense red-orange colours by historical sources (Rackham, 1968), which could be found in association with volcanic sublimates around fumaroles in its natural mineral form (Siddall, 2018). It was considered an "austere" pigment on artists' palettes of the Roman period as they knew that it turned to yellow pararealgar after intense exposure to light (Siddall, 2018).

It is worth noting that the FTIR spectrum (Fig. 3c) has absorption

bands at 2919 and 2851 ${\rm cm}^{-1}$, suggesting the presence of some organic compounds mixed with the realgar.

2.5. Yellow

Two yellow colours were preserved into the pots discovered in the House with Workshop (ref. 9642) and in the *domus* of Regio I 18, 2 (ref. 12013). Moreover, a pot containing a dull yellowish pigment (DOD1)

was also found in the *domus* with *atrium testidunatum* (VI 11, 11–12/7; Table 1). Under the microscope the sample ref. 9642 is compact with fine-sandy grain size, and it appears as a mixture of yellow particles (ca. 93%) including red (ca. 6%), blue (<1%) and white grains (<1%) (L* = 77.57; $a^* = 9.50$; $b^* = 45.23$; Table S1). The sample ref. 12 013 has a lighter shade (L* = 80.68; $a^* = 9.01$; $b^* = 41.16$), only containing white (ca. 3%) and blue particles (<1%). The sample DOD1 appeared as a fine-grained, compact yellowish powder in which white (ca. 11%),

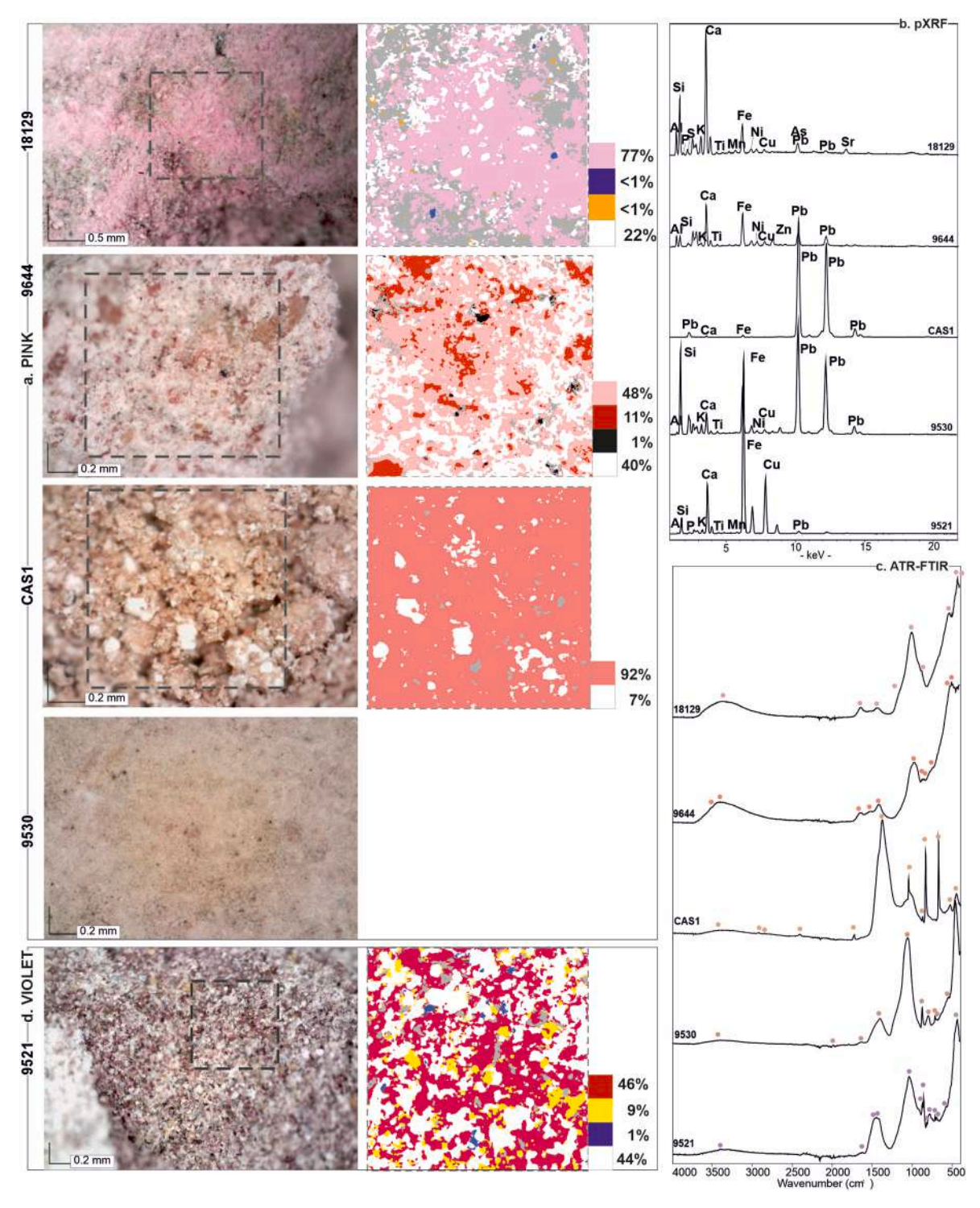


Fig. 4. a) DM images of pink pigments with results of DIA performed on representative areas. pXRF (b) and ATR-FTIR (c) spectra of pink and violet pigments. d) DM image of violet pigment with results of DIA performed on a representative area. (For interpretation of the references to colour in this figure legend, the reader is referred to the Web version of this article.)

reddish-brown (ca. 8 %) and black particles (ca. 4 %) can be observed (Fig. 3d).

From the chemical point of view, Fe is predominant, although Ca and Si were detected in moderate amounts (Fig. 3b). FTIR spectra (Fig. 3c-Table S1) are quite explicative for all samples, highlighting the occurrence of goethite (α -FeOOH) (ca. 3160, 1640, 910 and 796 cm⁻¹) (Guirdzhiiska et al., 2017) along with kaolinite (ca. 3692, 3650, 3619, 1113, 1028, 1004, 838, 753, 680, 635, 532, 465, 410 cm⁻¹), not detected in DOD1, and calcite (ca. 1410 cm⁻¹) (Germinario et al., 2022). These are the typical spectral features of yellow ochre, a pigment in which the goethite is the main colouring component and is naturally mixed with silicates and carbonates. Raman and FORS spectra support the hypothesis of the use of Fe-based pigments, showing the typical S-shape curve with the strong slope at ~580 nm, diagnostic of the yellow ochre (Marey Mahmoud, 2019) (Fig. S4) and Raman peaks of goethite at ca. 202, 240, 296, 351, 392, 481 and 548 cm⁻¹ (Froment et al., 2008) (Fig. S3). The reflectance curve of the sample DOD1, most clearly at \sim 460 nm, is typical of goethite (Fig. S4).

It is worth noting the presence of Pb in the sample DOD1 which was also detected in traces in the sample ref. 9642 (Table S1). If in the latter, the observation of red particles allowed us to justify the presence of Pb—likely added to increase the intensity of colour—as the addition of lead red (cerussa usta), in the sample DOD1 reddish-brown particles observed via DM seem to be a part of the yellowish matrix rather than an additional compound (Fig. 3d). In fact, the presence of Pb is quite unexpected in a sample containing goethite. However, Cottica and Mazzocchin (2009) also detected Pb in Pompeian yellow and gold-yellow pigments, raising the possibility of the occurrence of a low amount of lead compounds (i.e. white lead or yellow lead oxide) and such a hypothesis can actually be confirmed. The samples ref. 9642 and ref. 12013 also contain traces of Cu, likely related to the Egyptian blue particles (see below) observed via DM, whereas the sample DOD1 shows traces of Mn.

Based on the analytical data, we can confirm that the yellow pigments we analysed are earth-based pigments, namely *ochrae*, the most diffused yellow pigment in Pompeii (Aliatis et al., 2011; Augusti, 1967; Cottica and Mazzocchin, 2009; Giachi et al., 2009; Marcaida et al., 2018) or *sil*, in the case of the most precious variety (Table 2). However, the mineralogical composition of the sample DOD1 (i.e. predominance of goethite) could be due to a possible treatment of natural ochre (e.g., washing, levigation) (Eastaugh et al., 2008) that determined the enrichment of the pigment in iron hydroxides to the detriment to other natural compounds, such as clay minerals (Augusti, 1967).

It should be briefly noted that along with yellow ochre in Pompeii although As-based pigments, namely the orpiment (As₂S₃) called in antiquity *auripigmentum*, a Pb-based compound (PbO) (i.e., litharge) and a yellow madder from violet flowers to dye a white *creta* (Augusti, 1967) were also used. However, more recent studies also detected jarosite (KFe₃(SO₄)₂(OH)₆) as main constituent of yellow pigments (Baraldi et al., 2002; Fagnano et al., 2003; Giachi et al., 2009).

2.6. Pink

Four different shades of pink colour were investigated (Table 1). The pigment ref. 18129 has an unclear provenance (*Antiquarium*) whereas samples ref. 9644 and 9530 come from the House with Workshop. The sample CAS1, instead, was found during recent excavation of the room 2 in the House of Painters at Work.

The sample ref. 18129 contains three cubes of hard and compact pink pigment that, at higher magnification, appear composed of a very fine-grained groundmass with pink colour ($L^* = 71.76$; $a^* = 69.42$; $b^* = 63.64$) containing white (ca. 22 %), blue (<1 %) and orange (<1 %) grains (Fig. 4a). From the chemical point of view, the major elements are Ca, Si and Fe with moderate amounts of K, Al, Cu, As and Pb (Table S1; Fig. 4b).

Although Raman spectrum was affected by high fluorescence, FTIR

highlighted characteristic signals of pink organic pigments added to a silicate-bearing binder (3372, 1632, 1529, 1428, 999, 534, 426 cm⁻¹) (Fiocco et al., 2018; Papliaka et al., 2015) containing calcite (874 cm⁻¹) (Fig. 4c); this evidence was confirmed by FORS spectrum featured by the absorption band at ~500–580 nm typical of madder, which represents the organic compounds giving the pink colour. Two sub-bands peaking at 510–545 nm (Fig. S4) suggested the vegetal origin of madder (Aceto et al., 2014; Gulmini et al., 2013). Thus, the pink colour was obtained by dyeing an inorganic medium, probably composed of silicates and carbonate materials, with an organic colourant. In addition, ancient craftsmen added low amounts of (Cu-based) Egyptian blue and (As- and Pb-based) yellowish pigments to achieve a brighter hue.

This pigment can be identified with the purpurissum (Table 2), a pigment obtained by dyeing a colourless clay-rich substrate (creta) with shellfish (or murex) purple (Clarke et al., 2005; Cottica and Mazzocchin, 2009; Rackham, 1968), consistently with the results obtained by other authors on pink cubes found in Pompeii (Augusti, 1967; Clarke et al., 2005; Cottica and Mazzocchin, 2009; Giachi et al., 2009; Marcaida et al., 2018). In particular, on this sample, in-depth investigations carried out by Clarke and co-authors (Clarke et al., 2005) revealed the organic dye does not consist only of shellfish purple, but also alizarin, purpurin, indigotin and ellagic acid are contained in it. The addition of other materials to the shellfish purple (madder and some other plant colourant) had an implication on the final price of the pigment. In fact, it was counted among the high-priced artificial pigments (up to 30 denarii per pound) depending on how much true purple was used to make the pigment (Becker, 2022), considering that ca. 12 000 molluscs produced only about 1.4 g of dye (Friedländer, 1909). The use of a pigment derived from botanical sources was undoubtedly more cost-effective (Daniels et al., 2014).

The sample ref. 9644 shows a lighter shade (L* = 74.74; a* = 16.98; b* = 10.49). DM revealed a fine-sandy appearance with coarse light-to-dark reddish particles (up to 0.2 mm; ca. 11 %) with finer black grains (0.02 mm; ca. 1 %) scattered in a white matrix (ca. 40 %) showing pinkish areas (48 %) (Fig. 4a; Table S1). FTIR revealed the bands of silicate-bearing binder containing pink organic dye (3422, 1640, 1529, 1412, 970, 500 cm⁻¹) along with signals of calcite (1412, 872 cm⁻¹) and aragonite (850 cm⁻¹) (Fig. 4c; Table S1). The reflectance curve obtained by FORS also unveiled the organic compound, showing the typical band of the madder as in the previous sample and the absorption band at ~670 and ~870 nm common in the ochre (Fig. S4). However, pXRF (Fig. 4b) contributed to elucidate the composition of the mixture since the detection of Ca, Fe, Pb, and Si could be attributable to the addition of iron- and lead-based red pigment to the white (silicate- and carbonate-bearing) substrate, also dyed by adding an organic (madder) compound.

The sample ref. 9530, instead, is a very light pink pigment ($L^* = 78.21$; $a^* = 11.66$; $b^* = 15.83$) with a rather compact and cohesive appearance, resulting as a matrix in which whitish and yellowish areas can be observed along with dark red particles and abundant pearly white remains with an elongated shape, visible at higher magnification (Fig. 4a). Regarding the compounds giving the colour to the pigment, Giachi and co-authors assumed that it consisted in an organic dye. However, our data suggested that such a warmer shade was obtained by exclusively mixing pigments of inorganic nature, namely white earth containing diatomite, defined by Pliny as *creta argentaria* (Augusti, 1967; Rackham, 1968), with iron-based (*rubrica*) and lead-based red pigments (*cerussa usta*) (Table 2).

The sample CAS1 revealed another recipe for the pink shade (L* = 77.34; a* = 16.30; b* = 18.58). DM (Fig. 4a) revealed the presence of white (0.1–0.01 mm; 7 %) and warm pink particles (0.02–0.01 mm; 93 %), among which coarser dark red grains (up to 0.3 mm) can be identified (Table S3). As observed in the sample ref. 9530, pXRF (Fig. 4b; Table S1) detected prevalent Pb along with minor Fe and Ca. Vibrational spectroscopy unveiled the different origin of lead, along with a weak signal of calcite (876 cm $^{-1}$), FTIR showed the diagnostic bands of lead carbonate at 1730, 1379, 1051, 837 and 676 cm $^{-1}$ (Bishop et al., 2021)

(Fig. 4c), the presence of which was confirmed by Raman shifts at 1478, 1358, 1054, 841 and 679 cm⁻¹. Moreover, infrared bands of iron oxides at 530 and 453 cm⁻¹ (Farsang et al., 2021) (Fig. 4c), identified as hematite via RS (221, 292, 413 cm⁻¹) were observed (Table S1; Fig. S3). Interestingly, the FTIR spectrum also shows bands of organic compounds at 2924 and 2851 cm⁻¹ (C-H stretching vibration) that, unfortunately, we were not able to further discern even considering the FORS spectrum that only shows the diagnostic absorption bands of iron oxides (Fig. S4; Table S1). Thus, analytical data results revealed the addition of iron oxides (rubrica) in an inorganic binder constituted by lead white (cerussa), used to dilute the red hue until the desired pink hue was obtained (Table 2). In fact, cerussa, generally listed among the white pigments from historical sources (Morgan, 1960; Rackham, 1968), was occasionally found in Pompeian pigments as a dilutant to obtain clearer shades (Augusti, 1967; Baraldi et al., 2002; Giachi et al., 2009). However, it should be noted that the high concentrations of Pb detected in the pink lake pigments investigated by Marcaida and co-authors (Marcaida et al., 2016), despite the origin of lead, were certainly not confirmed.

2.7. Violet

The pot ref. 9521, found in the House with Workshop, keeps a small violet block ($L^* = 67.17$; $a^* = 4.00$; $b^* = 7.48$) that appears as a cohesive mixture of dark red (ca. 46 %), white (ca. 44 %), yellow (ca. 9 %) and rare blue grains (ca. 1 %) (Fig. 4d). Chemical composition of this mixture is featured by predominant Fe, moderate amounts of Cu, Ca, and Si, with lower Pb and K and traces of As (Table S1). FORS highlighted that the predominant iron is due to the red ochre, as the reflectance curve (Fig. S4) shows the band at ~580 nm, typical of this type of pigment. FTIR supported FORS data, revealing the bands of red ochre at 3360, 1626, 1038, 779, 695, 574, 434 cm⁻¹ (Fig. 4c). Moreover, peaks of calcite (1417, 873, 712 $\rm \,cm^{-1}$) and aragonite (1447, 855 $\rm \,cm^{-1}$) were also observed (Table S1). Thus, the colour was obtained by mixing inorganic pigments: the main component is the red ochre (rubrica), added to carbonate-bearing substrate (creta). However, microscopic observations and the presence of Pb, Cu and traces of As revealed a more complex recipe, obtained by adding red lead (cerussa usta), Egyptian blue (caeruleum, see below) and traces of orpiment (auripigmentum) as tone correctors (Table 2). This is the first report of a violet pigment obtained

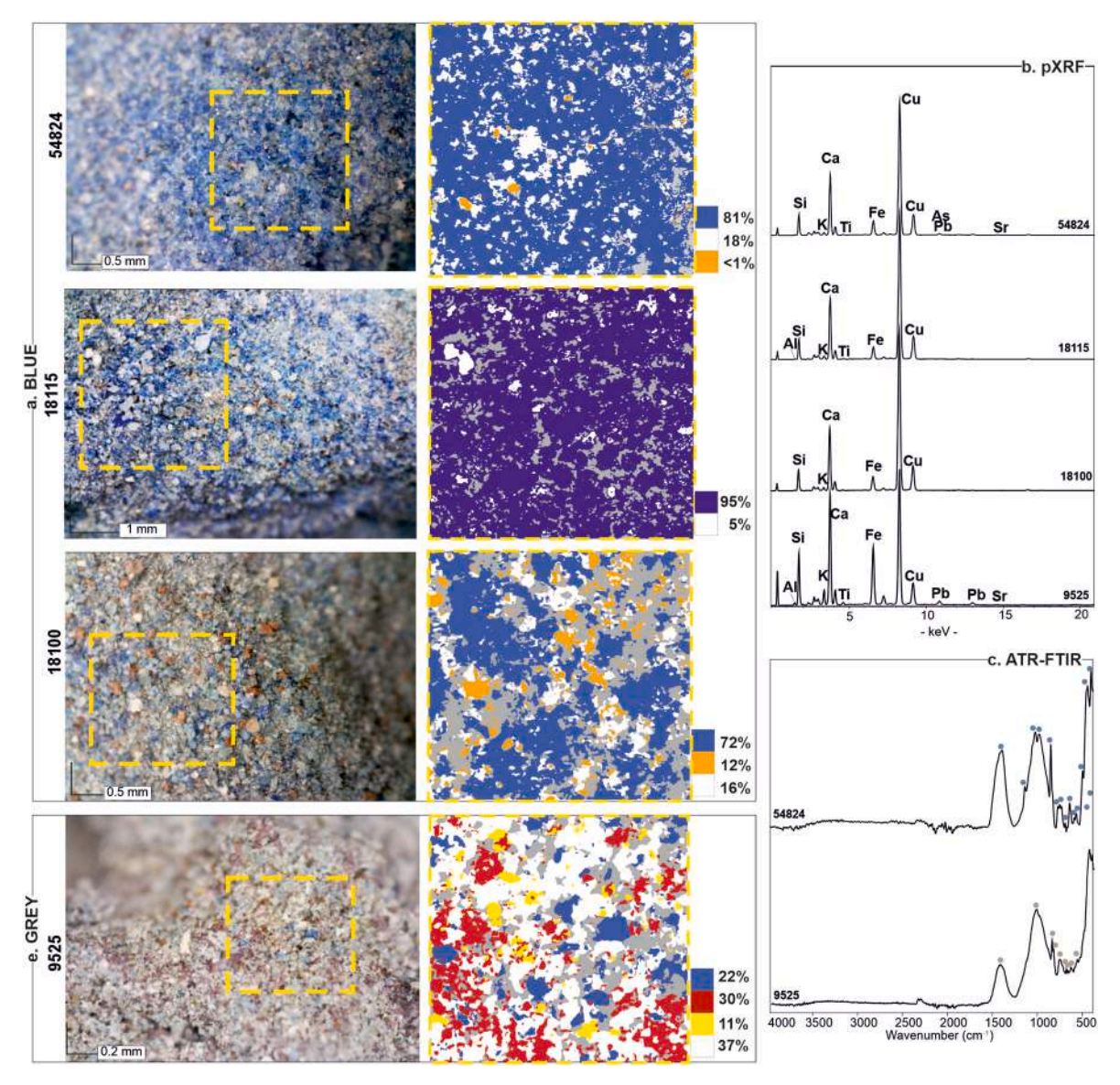


Fig. 5. a) DM images of blue pigments (refs. 54824, 18115, 18100), with results of DIA performed on representative areas (the blue areas also included grey, quartz and glass grains). pXRF (b) and representative ATR-FTIR (c) spectra of blue and grey pigments. d) DM image of grey pigment (ref. 9525) with results of DIA performed on a representative area. (For interpretation of the references to colour in this figure legend, the reader is referred to the Web version of this article.)

from a complex mixture of inorganic compounds at Pompeii, since all pigments with a violet shade so far investigated were obtained by using the *purpurissum* (Augusti, 1967; Cottica and Mazzocchin, 2009; Giachi et al., 2009; Marcaida et al., 2016). Only occasionally, the addition of Egyptian blue was observed to obtain the desired tonality (Marcaida et al., 2016).

2.8. Blue

Four pots containing blue pigment in powder form or in the shape of balls found in the House of the Queen of Netherlands (ref. 54824), from the *Antiquarium* (refs. 18115, 18100) and from the archaic layers of the Temple of Apollo (ref. 89129) were investigated. Moreover, blue powder from room 2 of the House of Painters at Work (sample CAS2) was collected on the 79 CE cinerite (Fig. 5a).

The different shades and colour measurements revealed different values of colourimetric coordinates: they vary from L* = 54.39; a* = -0.11; b* = -23.31 (ref. 54824) to L* = 67.20; a* = -5.92; b* = -4.13 in the lighter shade (ref. 18100) passing through intermediate values in the sample ref. 18115 (L* = 54.23; a* = -0.94; b* = -20.66) (Table S1). Colourimetric coordinates of the sample CAS2 (L* = 72.45; a* = -2.48; b* = -3.32) (Table S1), instead, reproduced a colour lighter than it really appears, probably because of the contact with the cinerite on which the pigment was found (Fig. S2).

Image analyses on DM micrographs (Fig. 5a) showed that the intensity of the blue colour depends on the abundance of blue particles. The latter were not quantified in the sample CAS2 because blue grains, with dimension ranging from 0.24 to 0.03 mm, were embedded in the cinerite (Fig. S2). The more intense blue pigment (ref. 18115) shows a predominance of blue particles with an average diameter of 0.09 mm (up to 95 %), mixed with white grains (ca. 5 %) (Fig. 5a; Table S2).

The number of blue grains decreases in pigment ref. 54824 (ca. 81 %) and featured a less intense shade, due to the presence of more abundant white grains (ca. 18 %) and sporadic orange spots (<1 %). The number of blue particles achieves values of ca. 72 % in the lighter blue hue (ref. 18100) (Fig. 5a), and in addition, the blue particles are finer (0.07 mm on average) and the resulting tone is influenced by the higher abundance of both white (ca. 16 %) orange particles (ca. 12 %) (Table S2). The blue grains (ranging from 0.24 to 0.04 mm) in the pot ref. 89129 are present in a lower percentage compared to other samples, combined with smaller white grains. However, they cannot be quantified, as they are spread out on the ceramic pot, as highlighted by the orange areas visible in DM images (Fig. S2).

The different appearance is reflected in the chemical data that revealed the abundance of copper, calcium, silicon and iron (Table S1), whose intensity in the pXRF spectra tends to reduce with the intensity of the colour. Interestingly, in the pigment ref. 18 100 As and Pb appear among the minor elements (Fig. 5b). This compositional evidence suggests the use of a copper-based blue pigment, confirmed by FTIR spectra (Fig. 5c) featured by the peaks at ca. 1160, 1045, 1002, 755, 663, 611, 590, 565, 520, 465, 424 cm⁻¹, characteristic of the Egyptian blue (Pagano et al., 2022), visible along with bands of calcite (ca. 1410, 872, 712 cm⁻¹) and aragonite (ca. 1470, 855 cm⁻¹), probably representing the white particles in the mixtures. Moreover, signals of quartz (ca. 795, 777, 695 cm⁻¹) are also detected, suggesting the presence of unreacted grains from the Egyptian blue production (Grifa et al., 2016), visible in DM images as scattered light grey particles (Fig. 5a), for the sake of clarity the quartz grains have been included in the blue pigment counts in digital image analyses.

RS and FORS confirm the presence of Egyptian blue as the main component, highlighting, respectively, the main Raman shift of cuprorivaite at $435~{\rm cm}^{-1}$ (Kostomitsopoulou Marketou et al., 2020) and the absorption bands at around $\sim\!630$ and $\sim\!800$ nm, together with a slope after $\sim\!580$ nm and the peak at 950 nm (Pagano et al., 2022) (Fig. S4).

Literature (Aliatis et al., 2011; Augusti, 1967; Baraldi et al., 2002;

Fagnano et al., 2003; Germinario et al., 2018b; Giachi et al., 2009; Marcaida et al., 2018; Siddall, 2006; Varone and Béarat, 1996) agrees that Egyptian blue, called *caeruleum* (a mixture of cuprorivaite, quartz, amorphous and other minor crystalline phases), is the main ingredient for the blue colours of Pompeii. It was even used as an additional compound for many other colours, and its extensive use was due to the presence of an active production district in the northern part of the *Campi Flegrei* (Grifa et al., 2016).

As demonstrated, the different nuances were obtained by mixing different proportions of Egyptian blue with other constituents, probably influencing the chemical and mineralogical composition of the mixture, whose variation cannot be undoubtedly attributed to different raw materials sources and/or alteration processes as a consequence of the burial, as stated by Marcaida and co-authors (Marcaida et al., 2018). In the Roman colour market, the different mixtures influenced the final price [up to 8 denarii per pound, according to Pliny (Rackham, 1968)]. However, the highest price was achieved for the lighter shades of the blue colour called *coelon*, obtained by finely grinding the *caeruleum*, and *lomentum* (10 denarii per pound) obtained by adding other substances (e.g., *creta*) to the finely ground *caeruleum* (Augusti, 1967).

If the GSD of blue pigments is considered (Fig. S5), samples refs. 18100, 18115 and 54824 are fine-grained. We suppose that ref. 18115 can be referred to *coelon* being only formed by Egyptian Blue pigment but, on the other hand, 54824 and 18100 are distinguished for the presence of additional Pb- and As- colouring substances, respectively, recalling the more precious *lomentum* (Table 2).

2.9. Grey

The grey colour of the sample ref. 9525 from the House with Workshop (L* = 60.53; a* = 3.11; b* = 4.23) appears as a fine powder (GDS from ca. 0.1 to 0.01 mm) with mixed white (ca. 37 %), dark red (ca. 30 %) and blue (ca. 22 %) particles along with minor yellow-orange (ca. 11 %) grains (Fig. 5d; Table S2). From a chemical point of view, the mixture is composed of abundant Cu and Ca, along with moderate amounts of Fe, Si, and K (Fig. 5b). It is worth pointing out that scarce traces of Pb and As were also detected (Table S1). FTIR spectrum shows the peaks featuring the Egyptian blue at ca. 1165, 1043, 1011, 786, 695, 664 592, 456, 424 cm $^{-1}$, along with peaks of calcite (ca. 1447, 872, 713 cm $^{-1}$) and the out-of-plane bending vibration of aragonite (ca. 853 cm $^{-1}$) (Table S1; Fig. 5c). FORS spectrum displays the \sim 650 and \sim 800 nm bands typical of Egyptian blue along with the slight \sim 550 nm band, likely attributed to the iron oxide particles (Fig. S4).

Thus, microscopic, compositional and spectral data illuminated the nature of a complex mixture, obtained by diluting Egyptian blue (*caeruleum*) with carbonates-bearing substances, likely associable to *creta* (calcite + aragonite); then, to obtain the desired greyish shade, iron-based (*rubrica*) and (minor) lead-based (*cerussa usta*) red pigments were added to the mixture along with very low amounts of yellowish arsenic-bearing pigment (*auripigmentum*) (Table 2).

Another mixture of a grey shade can be observed in pot ref. 18127, and impressively, the pot still contains two small blue pigment spheres and one light green sphere lying on a greyish material consisting of small light green (7 %), blue (28 %) and red grains (20 %) scattered in a finer matrix of greyish particles (45 %) (Fig. 6a).

The overall colorimetric coordinates (L* = 42.56; a* = -2.64; b* = 4.92) indicate a greyish hue; however, it is clearly distinguishable the contribution of the blue grains and light green with the characteristic absorbance at $\sim\!630$ and $\sim\!800$ nm (Fig. S4) and the red spots with absorbance at $\sim\!540$ and $\sim\!850$ nm (Fig. S4).

Interestingly, pXRF revealed a quite peculiar chemical composition; the technique detected high-intensity peaks of S, Ba, Fe and K along with minor Si, Al, Pb, Cu and Ca, (Fig. 6b). FTIR permitted preliminarily attributing such a chemical composition to mineral phases not detected in the other samples. In particular, along with infrared bands of Egyptian blue (1043, 1007, 599, 517, 454, 421 cm⁻¹), calcite (1461, 876 cm⁻¹)

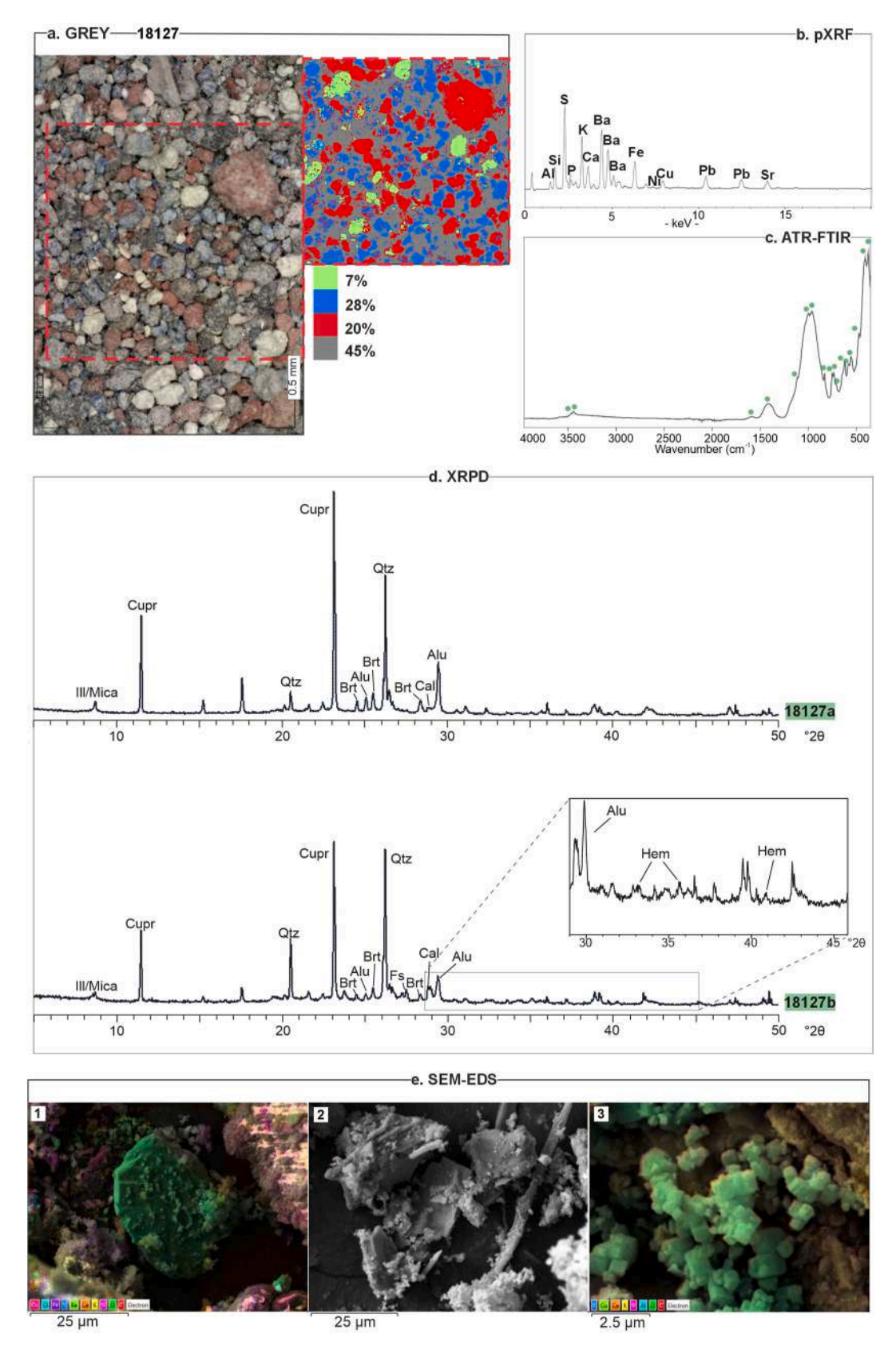


Fig. 6. a) DM images and results of DIA performed on representative areas. pXRF (b) and ATR-FTIR (c) spectra. d) Diffraction pattern (Abbreviations: Qtz, quartz; Ill/Mica, illite/mica; Cupr, cuprorivaite; Brt, baryte; Alu, alunite; Cal, calcite; Hem, hematite). e) SEM-EDS images performed on baryte (1), cuprorivaite (2), and alunite (3). Elemental maps of baryte and alunite.

and quartz (1165, 796, 779 cm $^{-1}$) (Table S1; Fig. 6c), the FTIR spectrum highlighted the presence of hydrated sulphates, namely alunite. Alunite, in fact, was recognised by the peaks at 3507, 3485 (O-H stretching vibration), 1626 (O-H bending vibration), 1079, 1030 ((SO₄)²⁻ asymmetric stretching vibration), 677, 625 ((SO₄)²⁻ asymmetric bending vibration) and 599 cm $^{-1}$ (O-H out-of-plane bending mode) (Murphy et al., 2009).

However, no signals of mineral phases containing Ba were clearly recognised via FTIR; thus, considering the quite atypical composition, we collected a few milligrams of the light green ball and grey mixture for a deeper investigation.

XRPD analyses further confirmed the mineralogical composition, showing that the light green ball (18127a Fig. 6d) is composed of i) baryte, a barium sulphate (BaSO₄) justifying the presence of Ba and S in pXRF; ii) quartz and cuprorivaite likely related to the Egyptian blue; iii) 10 Å phyllosilicates (i.e., Illite/Mica); iv) alunite, and v) traces of calcite (Fig. 6d). The grey material (18127b) shares the mineralogical composition of the light green ball with the addition of hematite (Fig. 6d).

Further, SEM/EDS maps allowed the elemental distribution and the micro-texture of any forming compound of this grey pigment to be observed. Baryte has a pseudo-prismatic habit with clear cleavage and particle size up to 30 μm (Fig. 6e1); cuprorivaite and quartz are clearly distinguishable for their chemical composition and share approximately the same grain size with baryte (Fig. 6e2); on the other hand, alunite appears as tiny pseudo-cubic crystals with a particle size of ca. 0.5 μm (Fig. 6e3).

All the acquired data reveals a rather unusual mineralogical and chemical composition for a Pompeian pigment; the current literature does not report a baryte- and alunite-bearing pigment among the colouring substances in the pots nor on the wall paintings.

For the sake of clarity, Aliatis and co-authors (Aliatis et al., 2009a) found alkaline sulphates (baryte and gypsum) as accessory minerals in red ochre in a Pompeian pigment pot, but they did not explain this peculiar feature. Baryte was also attested in Roman wall paintings in Rome from the excavations in the Monte d'Oro area (Guglielmi et al., 2022) and in wall paintings from two *villa rusticae* in Slovenia (Gutman et al., 2016) and these authors attributed the presence of barium sulphate as a natural impurity in red earth pigments.

Nevertheless, in our case, we can clearly state that baryte is one of the main compounds of the light green material (as a matter of fact, hematite only occurs in the grey mixture), demonstrating the first appearance of such a colouring material among the pigments in the Roman world and in the whole Mediterranean area.

It is worth noting that baryte, an extremely inert material used as a filler, was considered only after the experiments by Guyton de Morveau published in 1782 as a substitute for white lead, although the first mention of baryte (as a mineral) by Georg Agricola is dated to 1556 in *De Re Metallica* (Eastaugh et al., 2008).

2.10. Green

The green pigments (Fig. 7) in the pots ref. 41505 were found at House of the Painters at work, whereas 18 117 has uncertain provenance (Table 1). In particular, the sample ref. 41505 consists of a brilliant green powdered pigment (L* = 43.32; a* = -12.65; b* = 9.16) composed of green particles and traces of black grains; on the other hand, ref. 18117 is a dark green mixture (L* = 50.23; a* = -2.30; b* = 7.19) of green (ca. 80%), white (ca. 4%), red (ca. 7%), blue crystals (ca. 5%) and yellow grains (ca. 4%) (Fig. 7a).

Spectral features of green colours are distinctive for each sample. The

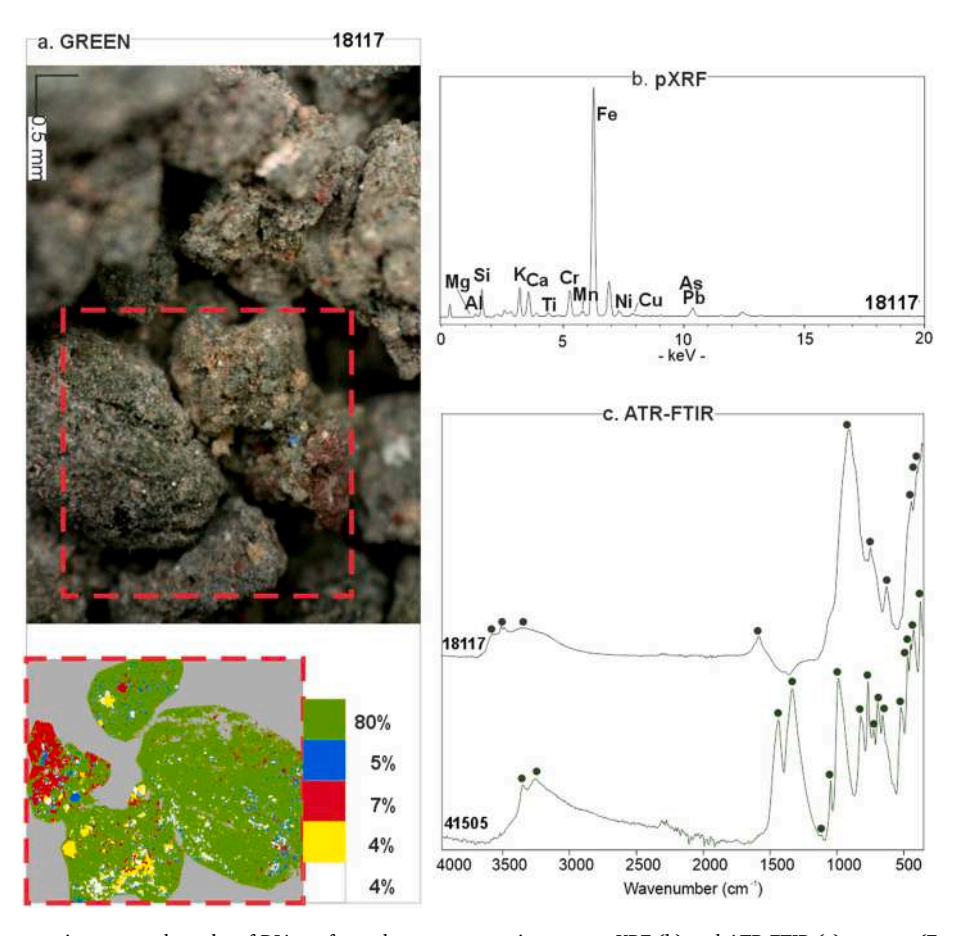


Fig. 7. a) DM images of green pigments and results of DIA performed on representative areas. pXRF (b) and ATR-FTIR (c) spectra. (For interpretation of the references to colour in this figure legend, the reader is referred to the Web version of this article.)

brilliant green colour (ref. 41505) shows the typical sharp bands of malachite (3394, 3302, 1484, 1382, 1163, 1096, 1038, 870, 816, 775, 745, 708, 571, 520, 498, 475, 425 cm⁻¹) (Aliatis et al., 2009a) (Table S1; Fig. 7c), as also confirmed by FORS that displays the typical reflectance spectrum featured by a wide absorption band from 600 to 900 nm (Cosentino, 2014).

This pigment, confirming previous studies performed on the same sample (Marcaida et al., 2018) was called *chrysocolla* or *armenium* in antiquity and was discussed at length by Pliny, who listed it as one of the most valuable pigments usually provided by the patron directly to the painter because of its preciousness (up to 7 denarii per pound) (Arena, 2020; Augusti, 1967).

On the other hand, the dark green mixture (ref. 18117) was composed of Fe, Cr as predominant elements, followed by K, Ca, Cu, Pb, Si and traces of As (Fig. 7b). FTIR spectrum shows distinct and sharp bands typical of celadonite at 3621, 3600, 3556, 3533, 3390, 1629, 955, 796, 676, 491, 449 cm⁻¹ (Aliatis et al., 2009b) (Fig. 7c; Table S1), as also confirmed by FORS that displays the characteristic spectrum of this phase, with the two peaks at \sim 560 nm and \sim 810 nm (Cheilakou et al., 2014) (Fig. S4).

Thus, the main constituent of the pigment is the green earth, in accordance with previous studies on the sample (Giachi et al., 2009). This compound was known in antiquity as *creta viridis*, a cheaper pigment that Pliny describes as "a pigment of scurvy price (1 sestertius per pound) (Arena, 2020) often used to imitate the more precious chrysocolla (*appianum*) falsely" (Augusti, 1967). However, the occurrence of blue, red and yellow particles suggests a more complex mixture; Giachi and co-authors (Giachi et al., 2009) report (red and yellow) iron oxides and copper blue in the mixture. The detection of Cu along with Pb and traces of As in our pXRF spectra could be indicative of the presence of copper- (blue), red- (lead) and arsenic-(yellow) pigments. Thus, we can suppose that the dark green nuance could be obtained by mixing the green earth (*creta viridis*) with minor particles of Egyptian blue (*caeru-leum*), red lead (*cerussa usta*) and orpiment (*auripigmentum*) (Table 2).

3. Discussion and conclusions

The Pompeian frescoes are invaluable for the study of Roman painting and provide an essential lens through which to understand the intersection of art, technology, and society in the Roman world. They offer a detailed record of artistic innovation, cultural practices, and social values, contributing to a more comprehensive understanding of ancient Roman visual culture and its enduring influence on subsequent artistic traditions in the Western world. This exceptional artistic process started with a wise selection of colouring materials, and Pompeii still offers unequivocal proof of this material culture.

In this study, strict criteria of sustainability were followed in the data acquisition to preserve the inestimable values of these archaeological materials; over the years, these pigments have attracted the interest of researchers and conservators and were on display at various exhibitions, resulting in a loss of material. Thus, the research was appropriately designed by combining information from complementary techniques to significantly advance knowledge on Pompeian pigments, achieving the three important goals described below.

3.1. The discovery of a new pigment mixture

The pigment contained in the pot ref. 18127 probably corresponds to the pot ref. 1637–4 analysed by Augusti (1967), in which he found two balls with two green shades (215A and 215B) and one blueish ball. However, probably due to analytical limitations, he gave this material a different composition, presenting a basic copper acetate (*aerugo*) and a lighter "washed and purified" green earth (*appianum*).

Our investigation revealed that the pot contains a grey pigment formulated by mixing a baryte- and alunite-bearing material with Egyptian blue and a red ochre. In this mixture, the two latter colouring compounds are well attested in the palette of ancient Roman artists; on the other hand, the sulphate deposit represents a novelty as an ingredient in the pigment's recipe.

Alunite and baryte occur in several environments of formation by supergene processes or hypogene alteration of sedimentary, igneous and metamorphic rocks. Alunite and baryte deposits next to Pompeii are limited to acid sulphate alteration environments in the Phlegraean Fields (Piochi et al., 2019) and Somma-Vesuvius (Balassone et al., 2019). Phleagraen alunite-rich deposits were exploited, from antiquity to recent periods, to produce alumen-(K) used in the tanning and dyeing industries and for medical purposes as well (Photos-Jones et al., 2016). This confirms that certain properties of these types of deposits were known; however, their specific use in a pigment mixture had not been previously documented.

However, large deposits are present close to Rome in the Allumiere-Tolfa volcanic complex, which contains several minerals of economic importance, including sulphates such as alunite and barite. These minerals result from intense post-volcanic supergene alteration of sulphidic minerals involving hydrothermal and meteoric water (Field and Lombardi, 1972), which affected the acidic (rhyolite) volcanic materials and a portion of the older underlying sedimentary rocks. In the Roman period, other spotted occurrences of baryte and alunite related to late hydrothermal activity can be associated with carbonatite systems in the Sabatini and Vulsini volcanic districts (Stoppa et al., 2019).

These sulphates are also associated with ore deposits, such as in Southern Tuscany, related to epithermal hypogene and supergene alteration (Dini, 2003), but might also be found as secondary minerals forming in sulfuric acid speleogenetic systems associated with carbonate rocks in karstic environments. These systems are widespread in Italy and, in some cases, can host diversified mineralogical associations, including alunite and baryte, as documented in caves in Umbria (Monte Cucco) and Sardinia (Corona 'e sa Craba) regions (D'Angeli et al., 2018).

Eventually, a deeper investigation will be conducted to provide new mineralogical and microchemical data to infer the origin and provenance of this material. In any case, its presence raises the need to compare it with mural paintings from other nearby contexts to understand whether this raw material was actually used or if its presence in Pompeii represents a unique case. Furthermore, the discovery of this pigment invites greater attention in the analysis of mural paintings. Having identified its use, the presence of sulfur on painted surfaces might not necessarily be associated with sulfation products, as is generally assumed, but could be due to a deliberate choice in the use of pigments.

3.2. Identifying the pigments' mixtures

The investigation strategy encompassed a wide range of analytical techniques to accurately identify the pigments by exploring their compositional and textural features.

The first important clue concerns the nature of the pigment(s); analytical results, in fact, revealed the absence of pure pigments, often reported in the previous studies on Pompeian pots (Aliatis et al., 2011; Augusti, 1967; Baraldi et al., 2002; Clarke et al., 2005; Cottica and Mazzocchin, 2009; Fagnano et al., 2003; Giachi et al., 2009; Marcaida et al., 2018; Varone and Béarat, 1996). All analysed samples constituted mixtures of two or more colouring compounds, likely in reply to specific artistic requirements. In this vein, two pigments seemed to play a fundamental role in the variation of colour tonality: Egyptian blue and red lead are almost ubiquitously observed as additional components in the pigments' mixtures.

Regarding Egyptian blue, a compound that has recently attracted significant attention leading to numerous applications (e.g., sensors, luminescent solar concentrators, energy-saving, biomedicine) among which is an innovative manufacturing process for producing cuprorivaite with increased NIR photoluminescence emission (Nicola et al., 2024), the literature largely reported that its addition for the production

of new colour tones was a standard Roman practice. Romans used a vast array of colours in their wall paintings and often the pigment mixtures contained Egyptian blue. For example, the addition of Egyptian blue to green and yellow earth produced a brighter green and yellowish shade, and its addition to iron-bearing pigments darkened the red colour to give them a brownish shade. A grey colour was obtained by desaturating the blue colour by adding small quantities of red iron oxides, and its mixture with white carbonates increased the white intensity by reducing the colour saturation in medium luminosity (Edreira et al., 2003).

However, the obtained shades also depended on the intensity of blue colour mixed to the other pigments. In fact, lighter or darker blue shades depended on the technology used for obtaining the pigment, in terms of a) firing time used by craftspeople during the production process (limited firing time prohibits the development of large cuprorivaite crystals, producing a lighter blue colour) (Delamare et al., 2004); b) grinding of blue particles to obtain finer grains (lightness of blue pigment increases with decreasing particle size) (Yang and Wan, 2020); and c) mixing with white pigments (i.e. creta and/or cerussa) (the addition of white compounds reduces the blue colour intensity) (Kostomitsopoulou Marketou et al., 2020). New analyses are ongoing on Egyptian Blue pigment samples by means of synchrotron micro-2d XRD mapping to clarify and detect any single compound and precisely quantify it to illuminate different production or preparation techniques.

Regarding red lead, the deliberate addition of this compound was made to adjust the hue of pigment, especially in the case of the colour red, and likely produced colour shades impossible to obtain with only one pigment. However, along with cinnabar, red ochre and red lake, its association with other pigments was only found in mixtures with lead white, calcite and black carbon (Gliozzo and Ionescu, 2021).

Until now, scholars have largely discussed mixtures of different pigments to achieve specific hues, but little attention has been paid to how the percentage of the different pigments affects the final colour shade. Our study demonstrated how the amount of one or the other determines the shade of the final colour towards blueish/greyish or reddish/violaceous tones. It was the case of grey (ref. 9525) and violet pigment (ref. 9521), in which we identified the same colouring compounds with significant differences in the amounts of Egyptian blue (22 % vs < 1 %) and red led (46 % vs 30 %) (Table S2).

3.3. Measuring the colour and quantifying colouring compounds in the mixtures

The research can be considered a pioneering study for an effective reconstruction of the technological practices of ancient artists in Pompeii's wall decoration. It contributes the most exciting advances in the "measurement of colour" in terms of quantification of the colourimetric parameters and colouring compounds despite the limiting operative conditions. In fact, in the long list of previous works on these pots, the authors only refer to the contents of the pigment pots in terms of the mineralogical (or other) composition of the main constituent, even in the case of pigment mixtures, never to the effective measurements of their colour.

Our approach revealed the composition of colouring compounds constituting the mixtures and quantified each compound to determine the amounts that ancient artists/artisans mixed together to achieve the desired colour and document the colorimetric coordinates of each shade. Pure pigments were not found, either in those colours (e.g. yellow), in which, at first glance, the colour appeared homogeneous.

Such an approach offers significant advantages for both the conservation and digital reconstruction of Pompeian wall paintings. By accurately identifying the compositions and proportions of materials used by ancient Roman artists—such as natural pigments, and binding agents—conservators could replicate mixtures that closely match the originals. This would improve the authenticity of modern conservation efforts, ensuring that restored sections of frescoes are chemically and visually consistent with the original works. Such knowledge could also

help reconstruct faded or damaged areas, preserving the frescoes' intended appearance and colour palette.

Moreover, this approach is crucial for the digital replication of Pompeian frescoes. Using colourimetric techniques, which measure precise colour and hue, researchers can digitally reconstruct the original vibrancy and tonal shifts of the frescoes, even in sections where the colours have faded. By integrating both colourimetric and microscopic and spectroscopic data, scholars can create digital models that simulate the exact colours and textures of the paintings as they would have appeared in antiquity, accounting for degradation over time. In addition to restoration, these digital reconstructions could be used to explore the evolution of Roman artistic techniques, the use of color in different social or architectural contexts, and how light interacted with painted surfaces. This digital approach not only aids in the conservation and understanding of Roman art but also makes it possible to present Pompeian frescoes in a historically accurate way, offering both scholarly and public audiences a deeper appreciation of ancient Roman visual culture.

CRediT authorship contribution statement

Celestino Grifa: Writing – review & editing, Writing – original draft, Supervision, Resources, Methodology, Investigation, Funding acquisition, Conceptualization. Chiara Germinario: Writing – review & editing, Writing – original draft, Visualization, Methodology, Investigation, Funding acquisition, Conceptualization. Sabrina Pagano: Writing – review & editing, Writing – original draft, Visualization, Investigation. Andrea Lepore: Writing – review & editing, Visualization, Investigation. Alberto De Bonis: Writing – review & editing, Resources, Methodology, Investigation. Mariano Mercurio: Writing – review & editing, Resources, Investigation. Vincenzo Morra: Writing – review & editing, Resources, Project administration. Gabriel Zuchtriegel: Writing – review & editing, Resources, Project administration. Sophie Hay: Writing – review & editing. Domenico Esposito: Writing – review & editing, Resources, Investigation.

Data and materials availability

All data are available in the main text or the supplementary materials.

Funding

This research was supported by:

Department of Science and Technology, University of Sannio grant FRA (CG, ChG, MM)

Declaration of competing interest

The authors declare that they have no known competing financial interests or personal relationships that could have appeared to influence the work reported in this paper.

Acknowledgments

The authors would like to thank Prof. Massimo Osanna for permission to investigate the pigment pots, Dr. Maria Francesca Alberghina and Dr. Salvatore Schiavone for supporting us in FORS measurements and Dr. Francesca d'Aniello for supporting us during pXRF measurements.

Appendix A. Supplementary data

Supplementary data to this article can be found online at https://doi. org/10.1016/j.jas.2025.106201.

References

- Aceto, M., Agostino, A., Fenoglio, G., Idone, A., Gulmini, M., Picollo, M., Ricciardi, P., Delaney, J.K., 2014. Characterisation of colourants on illuminated manuscripts by portable fibre optic UV-visible-NIR reflectance spectrophotometry. Anal. Methods 6, 1488–1500. https://doi.org/10.1039/c3ay41904e.
- Aliatis, I., Bersani, D., Campani, E., Casoli, A., Lottici, P.P., Mantovan, S., Marino, I.-G., Ospitali, F., 2009a. Green pigments of the Pompeian artists' palette. Spectrochim. Acta Part A Mol. Biomol. Spectrosc. 73, 532–538. https://doi.org/10.1016/j. saa.2008.11.009.
- Aliatis, I., Bersani, D., Campani, E., Casoli, A., Lottici, P.P., Mantovan, S., Marino, I., 2011. Pigments used in Roman wall paintings in the Vesuvian area. J. Raman Spectrosc. 41, 1537–1542.
- Aliatis, I., Bersani, D., Campani, E., Casoli, A., Lottici, P.P., Mantovan, S., Marino, I.G., Ospitali, F., 2009b. Green pigments of the Pompeian artists' palette. Spectrochim. Acta Part A Mol. Biomol. Spectrosc. 73, 532–538. https://doi.org/10.1016/j. saa.2008.11.009.
- Arena, G., 2020. Produzione di pigmenti pregiati in età imperiale: malattie "professionali" e maschere facciali. In: Commentaria Classica. Litterae Press, Catania, pp. 185–217.
- Augusti, S., 1967. I Colori Pompeiani. Rome.
- Balassone, G., Petti, C., Mondillo, N., Panikorovskii, T.L., de Gennaro, R., Cappelletti, P., Altomare, A., Corriero, N., Cangiano, M., D'Orazio, L., 2019. Copper minerals at Vesuvius volcano (southern Italy): a mineralogical review. Minerals. https://doi. org/10.3390/min9120730.
- Ballet, P., D'Auria, D., 2024. No TitleModes d'habiter à Pompéi à l'époque républicaine : diffusion et utilisation du type de la maison à atrium testudinatum. Bull. archéologique des Écoles françaises à l'étranger. https://doi.org/10.4000/baefe.10424.
- Baraldi, P., Fagnano, C., Ghittoni, A.L., Tassi, L., Zannini, P., 2002. Vibrational spectra of some pigments from Pompeii. AUTOMATA 1, 49–65. https://doi.org/10.1400/ 173336.
- Becker, H., 2022. Pigment nomenclature in the ancient near east, Greece, and Rome. archaeol. Anthropol. Sci. 14, 1–25. https://doi.org/10.1007/s12520-021-01394-1.
- Bishop, J.L., King, S.J., Lane, M.D., Brown, A.J., Lafuente, B., Hiroi, T., Roberts, R., Swayze, G.A., Lin, J.F., Sánchez Román, M., 2021. Spectral properties of anhydrous carbonates and nitrates. Earth Space Sci. 8. https://doi.org/10.1029/ 2021EA001844.
- Borgard, P., Brun, J.P., Tuffreau, M., Leguilloux, M., 2003. Le produzioni artigianali a Pompei. Richerche condotte dal Centre Jean Bérard. Riv. di Stud. pompeiani XIV 14, 9–29, 2003.
- Cheilakou, E., Troullinos, M., Koui, M., 2014. Identification of pigments on byzantine wall paintings from crete (14th century AD) using non-invasive fiber optics diffuse reflectance spectroscopy (FORS). J. Archaeol. Sci. 41, 541–555. https://doi.org/ 10.1016/j.jas.2013.09.020.
- Clarke, M., Frederick, P., Colombini, M.P., Andreotti, A., Wouters, J., van Bommel, M., Eastaugh, N., Walsh, V., Chaplin, T., Siddall, R., 2005. Pompei purpurissum pigment problems. In: Art 05: 8th International Conference on "Non-destructive Investigations and Microanalysis for the Diagnostics and Conservation of the Cultural and Environmental Heritage.", pp. 1–20.
- Coccato, A., Jehlicka, J., Moens, L., Vandenabeele, P., 2015. Raman spectroscopy for the investigation of carbon-based black pigments. J. Raman Spectrosc. 46, 1003–1015. https://doi.org/10.1002/jrs.4715.
- Cosentino, A., 2014. FORS Spectral Database of Historical Pigments in Different Binders, vols. 54–65. e-conservation J. https://doi.org/10.18236/econs2.201410.
- Cottica, D., Mazzocchin, G.A., 2009. Pots with coloured powders from the forum of Pompeii. In: 9th European Meeting on Ancient Ceramics, pp. 151–158.
- D'Angeli, I.M., Carbone, C., Nagostinis, M., Parise, M., Vattano, M., Madonia, G., Waele, J. De, 2018. New insights on secondary minerals from Italian sulfuric acid caves. Int. J. Speleol. 47, 271–291.
- Daniels, V., Devièse, T., Hacke, M., Higgitt, C., 2014. Technological insights into madder pigment production in Antiquity. Br. Museum 8.
- Delamare, F., Monge, G., Repoux, M., 2004. À la recherche de différentes qualités marchandes dans les bleus égyptiens trouvés à Pompéi. Riv. di Stud. Pompeiani 15, 89–107.
- Della Corte, M., 1965. Case ed abitanti di Pompei. Fausto Fiornetino Editore, Napoli.
- Dini, A., 2003. Ore deposits, industrial minerals and geothermal resources. Period. Mineral. 72, 41–52. https://doi.org/10.5038/1827-806X.47.3.2175.
- Eastaugh, N., Walsh, V., Chaplin, T., Siddall, R., 2008. Pigment Compendium: A Dictionary and Optical Microscopy of Historic Pigments. Butterworth-Heinemann, London.
- Edreira, M.C., Feliu, M.J., Fernández-Lorenzo, C., Martín, J., 2003. Spectroscopic study of Egyptian blue mixed with other pigments. Helv. Chim. Acta 86, 29–49. https:// doi.org/10.1002/hlca.200390017.
- Eschebach, H., 1993. Gebäudeverzeichnis und Stadtplan der antiken Stadt Pompeji. Böhlau Verlag Köln Weimar, Wien.
- Esposito, D., 2017. The economics of pompeian painting. In: Flohr, M., Wilson, A.I. (Eds.), The Economy of Pompeii (Oxford Studies on the Roman Economy). Oxford University Press, Oxford, pp. 261–288.
- Fagnano, C., Tinti, A., Taddei, P., Baraldi, P., 2003. La tavolozza dei colori negli affreschi di Pompei. In: Ricordo Di Alessandro Bertoluzza, pp. 1–13. https://doi.org/10.1400/ 33340
- Farsang, S., Widmer, R.N., Redfern, S.A.T., 2021. High-pressure and high-temperature vibrational properties and anharmonicity of carbonate minerals up to 6 GPa and 500 °C by Raman spectroscopy. Am. Mineral. 106, 581–598. https://doi.org/10.2138/ am-2020-7404.

- Field, C., Lombardi, G., 1972. Sulfur isotopic evidence for the supergene origin of alunite deposits, Tolfa district, Italy. Miner. Depos. 7, 113–125. https://doi.org/10.1007/ RE00207149
- Fiocco, G., Rovetta, T., Gulmini, M., Piccirillo, A., Canevari, C., Licchelli, M., Malagodi, M., 2018. Approaches for detecting madder lake in multi-layered coating systems of historical bowed string instruments. Coatings 8, 1–16. https://doi.org/ 10.3390/coatings8050171.
- Friedländer, P., 1909. Über den Farbstoff des antiken Purpurs aus murex brandaris. Berichte der Dtsch. Chem. Gesellschaft 42, 765–770. https://doi.org/10.1002/cber.190904201122.
- Froment, F., Tournié, A., Colomban, P., 2008. Raman identification of natural red to yellow pigments: ochre and iron-containing ores. J. Raman Spectrosc. 39, 560–568. https://doi.org/10.1002/jrs.1858.
- Germinario, C., Cultrone, G., De Bonis, A., De Simone, G.F., Gorrasi, M., Izzo, F., Langella, A., Martucci, C.S., Mercurio, M., Morra, V., Vyhnal, C.R., Grifa, C., 2021. Production technology of late roman decorated tableware from the Vesuvius environs: evidence from pollena trocchia (campania region, Italy). Geoarchaeology 36, 34–53. https://doi.org/10.1002/gea.21819.
- Germinario, C., Cultrone, G., De Bonis, A., Izzo, F., Langella, A., Mercurio, M., Morra, V., Santoriello, A., Siano, S., Grifa, C., 2018a. The combined use of spectroscopic techniques for the characterisation of Late Roman common wares from Benevento (Italy). Measurement 114, 515–525. https://doi.org/10.1016/j.measurement.2016.08.005.
- Germinario, C., Izzo, F., Mercurio, M., Langella, A., Sali, D., Kakoulli, I., De Bonis, A., Grifa, C., 2018b. Multi-analytical and non-invasive characterization of the polychromy of important archaeological wall paintings at the Domus of Octavius Quartio in Pompeii. Eur. Phys. J. Plus 133, 359. https://doi.org/10.1140/epjp/i2018-12224-6.
- Germinario, C., Pagano, S., Mercurio, M., Izzo, F., De Bonis, A., Morra, V., Munzi, P., Leone, M., Conca, E., Grifa, C., 2022. Roman technological expertise in the construction of perpetual buildings: new insights into the wall paintings of a banquet scene from a tomb in Cumae (southern Italy). Archaeol. Anthropol. Sci. 14. https:// doi.org/10.1007/s12520-022-01651-x.
- Giachi, G., De Carolis, E., Pallecchi, P., 2009. Raw materials in pompeian paintings: characterization of some colors from the archaeological site. Mater. Manuf. Process. 24, 1015–1022. https://doi.org/10.1080/10426910902982631.
- Gliozzo, E., Ionescu, C., 2021. Pigments—lead-based whites, reds, yellows and oranges and their alteration phases. Archaeol. Anthropol. Sci. 14, 17. https://doi.org/ 10.1007/s12520-021-01407-z.
- Grifa, C., Cavassa, L., De Bonis, A., Germinario, C., Guarino, V., Izzo, F., Kakoulli, I., Langella, A., Mercurio, M., Morra, V., Lloyd, I., 2016. Beyond vitruvius: new insight in the technology of Egyptian blue and green frits. J. Am. Ceram. Soc. 99, 3467–3475. https://doi.org/10.1111/jace.14370.
- Guglielmi, V., Andreoli, M., Comite, V., Baroni, A., Fermo, P., 2022. The combined use of SEM-EDX, Raman, ATR-FTIR and visible reflectance techniques for the characterisation of Roman wall painting pigments from Monte d'Oro area (Rome): an insight into red, yellow and pink shades. Environ. Sci. Pollut. Res. 29, 29419–29437. https://doi.org/10.1007/s11356-021-15085-w.
- Guirdzhiiska, D., Zlateva, B., Glavcheva, Z., 2017. Polished decorative Fields in thracian fresco tombs from the hellenistic period - archaeometrical research. Sci. Technol. Archaeol. Res. 3, 428–436. https://doi.org/10.1080/20548923.2017.1396723.
- Gulmini, M., Idone, A., Diana, E., Gastaldi, D., Vaudan, D., Aceto, M., 2013. Identification of dyestuffs in historical textiles: strong and weak points of a non-invasive approach. Dyes Pigments 98, 136–145. https://doi.org/10.1016/j.dvepig.2013.02.010.
- Gutman, M., Zanier, K., Lux, J., Kramar, S., 2016. Pigment analysis of roman wall paintings from two villae rusticae in Slovenia. Mediterr. Archaeol. Archaeom. 16, 193–206. https://doi.org/10.5281/zenodo.160970.
- Izzo, F., Germinario, C., Grifa, C., Langella, A., Mercurio, M., 2020. External reflectance FTIR dataset (4000–400 cm-1) for the identification of relevant mineralogical phases forming Cultural Heritage materials. Infrared Phys. Technol. 106, 103266. https://doi.org/10.1016/j.infrared.2020.103266.
- Kostomitsopoulou Marketou, A., Andriulo, F., Steindal, C., Handberg, S., 2020. Egyptian blue pellets from the first century BCE workshop of kos (Greece): microanalytical investigation by optical microscopy, scanning Electron microscopy-X-ray energy dispersive spectroscopy and micro-Raman spectroscopy. Minerals 10. https://doi. org/10.3390/min10121063.
- Marcaida, I., Maguregui, M., Morillas, H., García-Florentino, C., Knuutinen, U., Carrero, J.A., Fdez-Ortiz De Vallejuelo, S., Pitarch Martí, A., Castro, K., Madariaga, J. M., 2016. Multispectroscopic and isotopic ratio analysis to characterize the inorganic binder used on pompeian pink and purple lake pigments. Anal. Chem. 88, 6395–6402. https://doi.org/10.1021/acs.analchem.6b00864.
- Marcaida, I., Maguregui, M., Morillas, H., Prieto-Taboada, N., de Vallejuelo, S.F.-O., Veneranda, M., Madariaga, J.M., Martellone, A., De Nigris, B., Osanna, M., 2018. In situ non-invasive characterization of the composition of Pompeian pigments preserved in their original bowls. Microchem. J. 139, 458–466. https://doi.org/ 10.1016/j.microc.2018.03.028.
- Marey Mahmoud, H.H., 2019. Colorimetric and spectral reflectance access to some ancient Egyptian pigments. J. Int. Colour Assoc. 35–45.
- Morgan, N.H., 1960. Vitruvius. The Ten Books on Architecture. Dover Publications, New York.
- Murphy, P.J., Smith, A.M.L., Hudson-Edwards, K.A., Dubbin, W.E., Wright, K., 2009. Raman and ir spectroscopic studies of alunite-supergroup compounds containing Al, Cr3+, Fe3+ AND V3+ at the B site. Can. Mineral. 47, 663–681. https://doi.org/10.3749/canmin.47.3.663.

- Nicola, M., Garino, C., Mittman, S., Priola, E., Palin, L., Ghirardello, M., Damagatla, V., Nevin, A., Masic, A., Comelli, D., Gobetto, R., 2024. Increased NIR photoluminescence of Egyptian blue via matrix effect optimization. Mater. Chem. Phys. 313, 128710. https://doi.org/10.1016/j.matchemphys.2023.128710.
- Pagano, S., Germinario, C., Alberghina, M.F., Covolan, M., Mercurio, M., Musmeci, D., Piovesan, R., Santoriello, A., Schiavone, S., Grifa, C., 2022. Multilayer technology of decorated plasters from the domus of marcus vipsanus primigenius at abellinum (campania region, southern Italy): an analytical approach. Minerals. https://doi.org/ 10.3390/min12121487.
- Papliaka, Z.E., Konstanta, A., Karapanagiotis, I., Karadag, R., Akyol, A.A., Mantzouris, D., Tsiamyrtzis, P., 2015. FTIR imaging and HPLC reveal ancient painting and dyeing techniques of molluskan purple. Archaeol. Anthropol. Sci. 9, 197–208. https://doi. org/10.1007/s12520-015-0270-3.
- Photos-Jones, E., Christidis, G.E., Piochi, M., Keane, C., Mormone, A., Balassone, G., Perdikatsis, V., Leanord, A., 2016. Testing Greco-Roman medicinal minerals: the case of solfataric alum. J. Archaeol. Sci. Reports 10, 82–95. https://doi.org/ 10.1016/j.jasrep.2016.08.042.
- Piochi, M., Mormone, A., Strauss, H., Balassone, G., 2019. The acid sulfate zone and the mineral alteration styles of the Roman Puteoli (Neapolitan area, Italy): clues on fluid fracturing progression at the Campi Flegrei volcano. Solid Earth 10, 1809–1831. https://doi.org/10.5194/se-10-1809-2019.
- Rackham, H., 1968. Pliny the elder. Natural History in Ten Volumes. Harvard University Press. Cambridge.
- Salvadori, M., Sbrolli, C., 2021. Wall paintings through the ages: the roman period—republic and early Empire. Archaeol. Anthropol. Sci. 13, 187. https://doi. org/10.1007/s12520-021-01411-3.
- Siddall, R., 2018. Mineral pigments in archaeology: their analysis and the range of available materials. Minerals. https://doi.org/10.3390/min8050201.

- Siddall, R., 2006. Not a day without a line drawn: pigments and painting techniques of Roman Artists. infocus Mag 18–31. https://doi.org/10.22443/rms.inf.1.4.
- Stoppa, F., Schiazza, M., Rosatelli, G., Castorina, F., Sharygin, V.V., Ambrosio, F.A., Vicentini, N., 2019. Italian carbonatite system: from mantle to ore-deposit. Ore Geol. Rev. 114, 103041. https://doi.org/10.1016/j.oregeorev.2019.103041.
- Tomasini, E., Halac, E., Reinoso, M., Di Liscia, E., Maier, M., 2012a. Micro-Raman spectroscopy of carbon-based black pigments. J. Raman Spectrosc. 43, 1671–1675.
- Tomasini, E., Siracusano, G., Maier, M.S., 2012b. Spectroscopic, morphological and chemical characterization of historic pigments based on carbon. Paths for the identification of an artistic pigment. Microchem. J. 102, 28–37. https://doi.org/ 10.1016/j.microc.2011.11.005.
- Tuffreau-Libre, M., Brunie, I., Daré, S., 2014. L'artisanat de la peinture à Pompéi. Chron. des Act. archéologiques l'École française Rome. https://doi.org/10.4000/cefr.1205.
- Varone, A., 1995. L'organizzazione del lavoro di una bottega di decoratori: le evidenze dal recente scavo pompeiano lungo via dell' Abbondanza. Meded. van het Ned. Inst. te Rome, Antiq. 54, 124–136.
- Varone, A., Béarat, H., 1996. Pittori romani al lavoro. Materiali, strumenti, tecniche: evidenze archeologiche e dati analitici di un recente scavo pompeiano lungo Via dell'Abbondanza (Reg. IX Ins.12). In: International Workshop on Roman Wall Painting. Fribourg, pp. 199–214.
- Vermeulen, M., Saverwyns, S., Coudray, A., Janssens, K., Sanyova, J., 2018. Identification by Raman spectroscopy of pararealgar as a starting material in the synthesis of amorphous arsenic sulfide pigments. Dyes Pigments 149, 290–297. https://doi.org/10.1016/j.dyepig.2017.10.009.
- Yang, X.-L., Wan, X.-X., 2020. Analysis of the spectral reflectance and color of mineral pigments affected by their particle size. Color Res. Appl. 45, 246–261. https://doi. org/10.1002/col.22455.